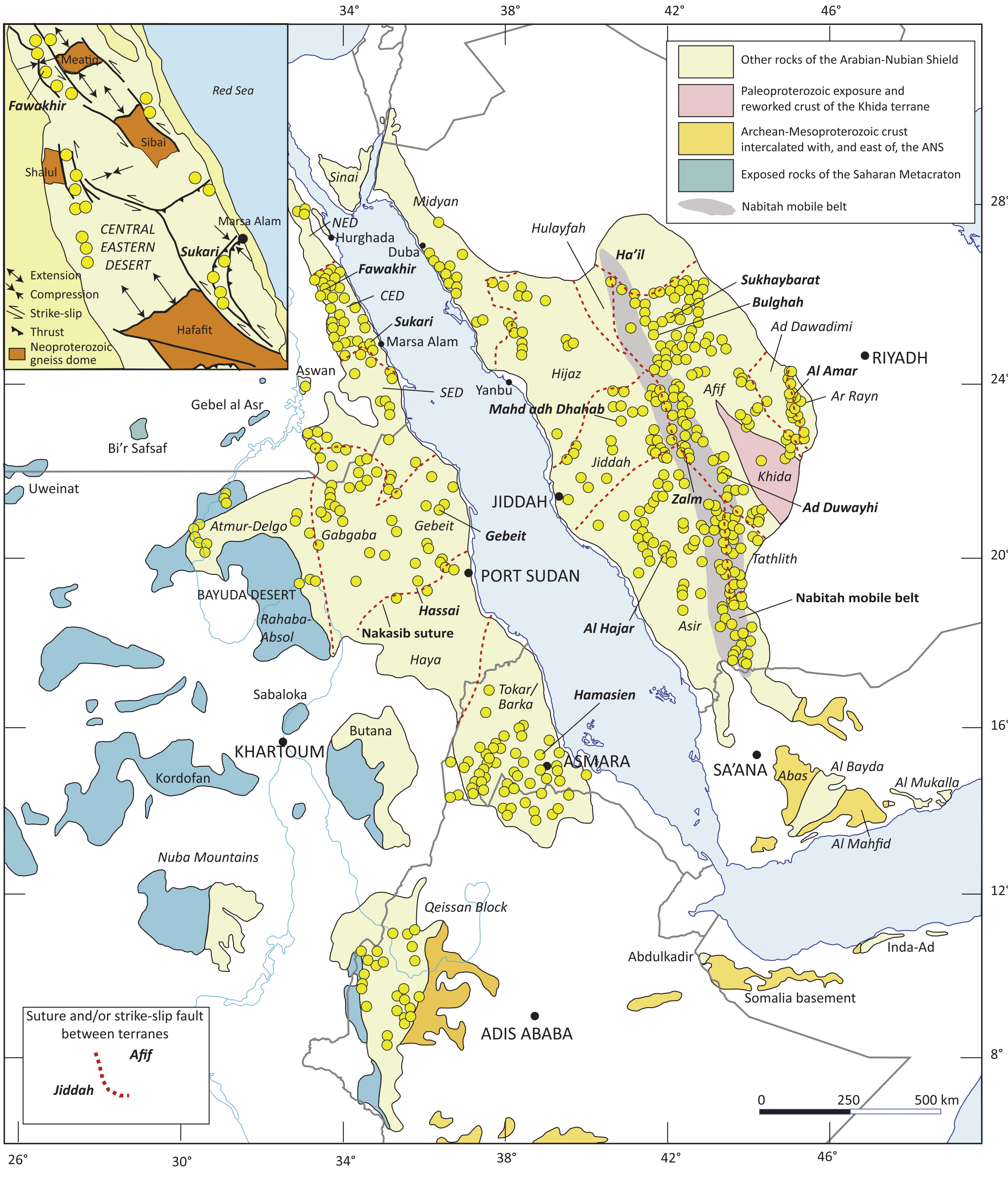

Fig. 23. Simplified plot of gold occurrences in the Arabian–Nubian Shield, showing their wide distribution throughout the region. The occurrences are predominantly late Cryogenian–Ediacaran orogenic-type gold in a variety of structural and lithologic settings, but include epithermal deposits (Mahd adh Dhahab, Al Amar), some VMS-gold, and carbonate-altered ultramafic-associated gold. After Saudi Arabian Mineral Occurrence Documentation System (for the Arabian Shield); Botros (2002) (for the Eastern Desert, Egypt); Klemm et al. (2001) (for northern Sudan); Tadesse et al. (2003) (for Ethiopia); Jelenc (1966) for Eritrea. Major deposits are named. Important orogenic-gold occurrences in Ethiopia, e.g., Lega-Dembi, are in the Adola Belt, at about 5°N, south of the present figure. Inset, after Helmy et al. (2004) as an example of the structural control on orogenic-type deposits.

dikes that connect with a larger sill about 100 m below the surface. Mineralization consists of wolframite, cassiterite, scheelite, and molybdenite in quartz veins and phyllic-altered microgranite and developed in three phases: early quartz-molybdenite stockwork veining; wolframite- and scheelite-bearing, greisen-bordered veining; and late quartz–carbonate–fluorite veining. U–Pb analysis of zircon from a quartz vein gives an approximate age of 575 Ma (Stacey and Stoeser, 1984), which is consistent with mineralization at the time of granite emplacement. Fluid inclusions and oxygen isotope data indicate that the deposit formed over a temperature range of 120–550 °C, from low salinity magmatic and metamorphic fluids, and at a depth of about 4.2 km (Kamilli et al., 1993). Eighteen shallow percussion drill holes in the northern part of the occurrence outline a resource of 800,000 t of quartz-veined microgranite containing 0.090–0.117% WO_3 and 0.007–0.012% Sn, and the whole occurrence is estimated to be about 10 Mt.

8.2.3. Other types of granitoid-associated mineralization

Other types of late Cryogenian–Ediacaran granitoid-associated mineralization in the Arabian Shield include Ujaiyah (Khushaymiyah) (Mo–W–Bi), Bi'r Tawilah (W–Mo–Sn), and the Ad Dawadimi silver district (Pb–Zn–Ag), as well as a mineralized breccia pipe (Ablah-F), REE-bearing pegmatites and silexites, and contact Fe-replacement deposits associated with alkali-feldspar syenite, quartz alkali-feldspar syenite, quartz syenite, and particularly their fine-grained apical variants.

The *Ujaiyah* prospect is hosted by the Kushaymiyah batholith (611 ± 3 Ma; Agar et al., 1992) up to 50 km across, made up of as many as ten overlapping subcircular plutons of monzogranite and granodiorite, each 10–15 km in diameter. The batholith intrudes the Murdama group, and septa of Murdama rock are incorporated in the southeastern margin of the batholith. Mineralization is focused on the Thaaban pluton in the southeastern part of the batholith. The pluton is a ring complex with a core of quartz monzonite, an outer zone of granodiorite, and an outermost ring of younger quartz monzonite. The core is cut by a quartz vein swarm emplaced in pervasively sericitized and greisenized quartz monzonite. The veins carry disseminated pyrite, molybdenite, and scheelite with minor galena, chalcopyrite, and bismuthinite. The margin of the pluton has veins with Pb, Zn, Cu, and Ag. Metal values are low (averaging 80 ppm Mo in samples of quartz vein and host rock; and 430 ppm in veins alone), and no serious investigation has been conducted since early work by the USGS Saudi Arabian Mission (Dodge and Helaby, 1974).

The *Bi'r Tawilah* intrusion is a polyphase body of quartz leucodiorite, porphyritic biotite granodiorite, microgranodiorite, fine-grained porphyritic granite, and veins of albite microgranite (Collenette and Grainger, 1994). The intrusion was emplaced in sericite–quartz–chlorite schist immediately east of the Bi'r Tawilah thrust. Mineralization consists of aggregates and disseminations of wolframite, cassiterite, traces of base-metal sulfides, and pyrite in quartz veins in the intrusion and wall rock. Grades in the western part of the occurrence average 0.69% WO_3, 0.13% Sn, and 26 g/t Ag. Bi'r Tawilah tungsten was a primary focus of exploration in the area until a greater importance of gold was recognized.

The *Ad Dawadimi* silver district (Al-Shanti, 1976; Collenette and Grainger, 1994) comprises Pb–Zn–Ag mineralized quartz veins, which are similar to orogenic mesothermal gold veins in other parts of the shield but unique in that silver is the main economic metal. The district is in the heart of the Ad Dawadimi terrane in the eastern part of the shield centered on the town of Ad Dawadimi. The veins, many the site of ancient workings, crop out in an area of about 30 km N–S and 10 km E–W. Most of the mineralized veins, which trend either NW or NE, are in shear zones in a biotite monzogranite–granodiorite–quartz monzodiorite batholith or layered gabbro. The main silver minerals are polybasite, pyrargyrite, and freibergite, in association with galena and subordinate sphalerite. The wall rocks are extensively brecciated and pervasively affected by propylitic and weak phyllic alteration. The reason for such a concentration of silver-mineralized veins in this part of the shield is not known. Al-Shanti (1976) concluded that the mineralization was controlled by: (1) emplacement of the granite batholith; (2) Najd faulting which produced suitable host structures; and (3) the presence of Abt-formation argillaceous sedimentary inclusions in the batholith. During early investigations, only eight occurrences yielded results that justified drilling, and of the eight, only one (Samrah) is of any significance, with an estimated resource of 278,000 t grading 653 g/t Ag, 5.12% Zn, and 1.64% Pb.

Ablah, in the northwestern part of the Asir terrane, is the largest late Cryogenian–Ediacaran fluorite occurrence known in the ANS (Collenette and Grainger, 1994). It consists of massive fluorite and veins and pods of Cu-, Pb-, Zn-, and Ag-sulfides in a breccia pipe up to 22 m in diameter. The pipe is emplaced in a pegmatite–aplite breccia 300 m long and 130 m wide, which in turn is emplaced in a diorite host. *Jabal Hamra*, in the Hijaz terrane, is a lenticular vertical body of fine-grained silexite, an igneous rock composed essentially of primary quartz (60–100%), intruded into a quartz-alkali-feldspar syenite. The pipe carries disseminations of Nb-, Ta-, Sn-, REE-, Y-, Th-, U-, and Zr-bearing minerals and the host syenite contains pegmatite with Nb, Zr, Y, and REE minerals.

8.3. Late Cryogenian–Ediacaran arc-related mineralization

A distinctive suite of late Cryogenian–Ediacaran mineral occurrences are found in the Ar Rayn terrane in the easternmost ANS (Doebrich et al., 2007). They represent convergent-margin deposits of the type that elsewhere in ANS are associated with the older early-middle Cryogenian magmatic arcs but continued into the late Cryogenian–Ediacaran in the Al Amar arc because of ongoing >689–615 Ma subduction. The most notable occurrences are Al Amar, a polymetallic epithermal deposit, and Khnaiguiyah, a major Zn–Cu sulfide deposit (see references in Sangster and Abdulhay, 2005). Neither occurrence is dated, but mineralization is believed to be either approximately the same age or somewhat younger than the >689–615 Ma Al Amar-arc host rocks.

The *Al Amar* deposit comprises polymetallic and gold-bearing veins, subordinate massive sulfides, and beds and lenses of exhalative talc, barite, and Ca–Fe–Mn carbonates located a few hundred meters east of the Al Amar fault. The Al Amar host rocks include mafic to intermediate pyroclastic rocks and subordinate andesite flows; felsic volcaniclastic rocks and lava, subordinate red jasper, and polymict conglomerate; and felsic to intermediate tuffs and pyroclastic flows. The principal veins occur in two subvertical, northwest-trending zones referred to as the North and South Veins. They extend on the surface as much as 500 m along strike, discordant to the bedding, and to depths of at least 350 m. The veins are composed of quartz and subordinate Ca–Fe–Mn carbonates, barite, anhydrite, and sulfides (pyrite, sphalerite, chalcopyrite, and galena). Gold is locally free but mainly occurs as Au–Ag tellurides and electrum in the sulfides. Massive sulfide ore consists of sphalerite, barite, chalcopyrite, talc, carbonate, and chlorite, and probably originated during a period of volcanic quiescence. Doebrich et al. (2007) refer to the vein mineralization as epithermal, whereas Sangster and Abdulhay (2005) use the terms "structurally controlled, epigenetic". Pouit et al. (1984) interpret the massive sulfide mineralization as a volcanogenic exhalative deposit coeval with the formation of the Al Amar group. The deposit is in production, and as of mid-2007, had a reserve of 1.4 Mt ore grading 9.9 g/t Au, and total mineral resources comprising 2.0 Mt grading 11.2 g/t Au (SRK Consulting, 2007).

Khnaiguiyah is a sulfide deposit of uncertain origin in strongly sheared rocks in the northern part of the Ar Rayn terrane. It consists of four stratiform lenses of magnetite, hematite, pyrite, sphalerite, chalcopyrite, rhodochrosite, rhodonite, Ag-, Pb- and Bi-tellurides, and barite in carbonate-altered shear zones. The orebodies are hosted by discontinuous anastomosing bands of carbonatized rock in rhyolitic and subordinate andesitic rocks of

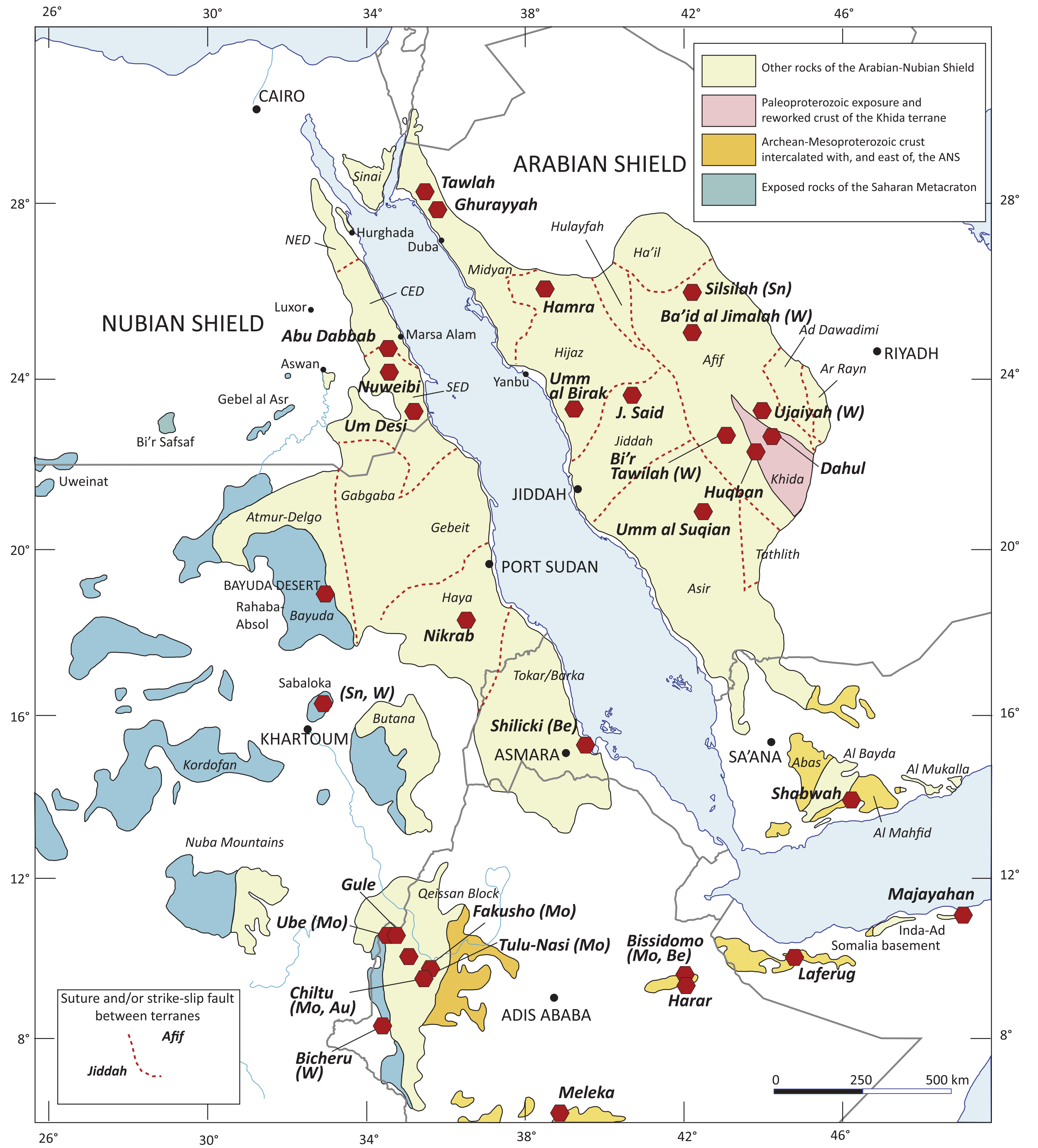

Fig. 24. Refractory and other special metal occurrences associated with late- to posttectonic, A-type granites, peraluminous granites, and localy pegmatites in the Arabian–Nubian Shield, after Saudi Geological Survey Mineral Occurrence Documentation System and Drysdall et al. (1984) (for the Arabian shield), Küster (2009) for Egypt, Sudan, and Somalia; and Jelenc (1966) and Tadesse et al. (2003) for Ethiopia and Eritrea. Occurrences are Ta–Nb–U rich unless otherwise indicated.

the Al Amar group. Alternative interpretations of the deposit are that it is a hydrothermal exhalation contemporary with the enclosing volcanic rocks—a type of VMS deposit (Testard, 1983), or that it is the result of hydrothermal alteration along post-metamorphic, posttectonic shear zones (BRGM Geoscientists, 1993). The Zn grades range between <5% and 33% and Cu grades range up to 1.5%. Resource figures published by BRGM Geoscientists (1993) indicate a "drill-measured total resource" of 24.8 Mt grading 4.11% Zn, 0.56% Cu.

8.4. Mafic-pluton associated mineralization

The *Lakathah* complex in the southwestern Arabian Shield (Martin et al., 1979) is a nearly circular posttectonic ring-dike

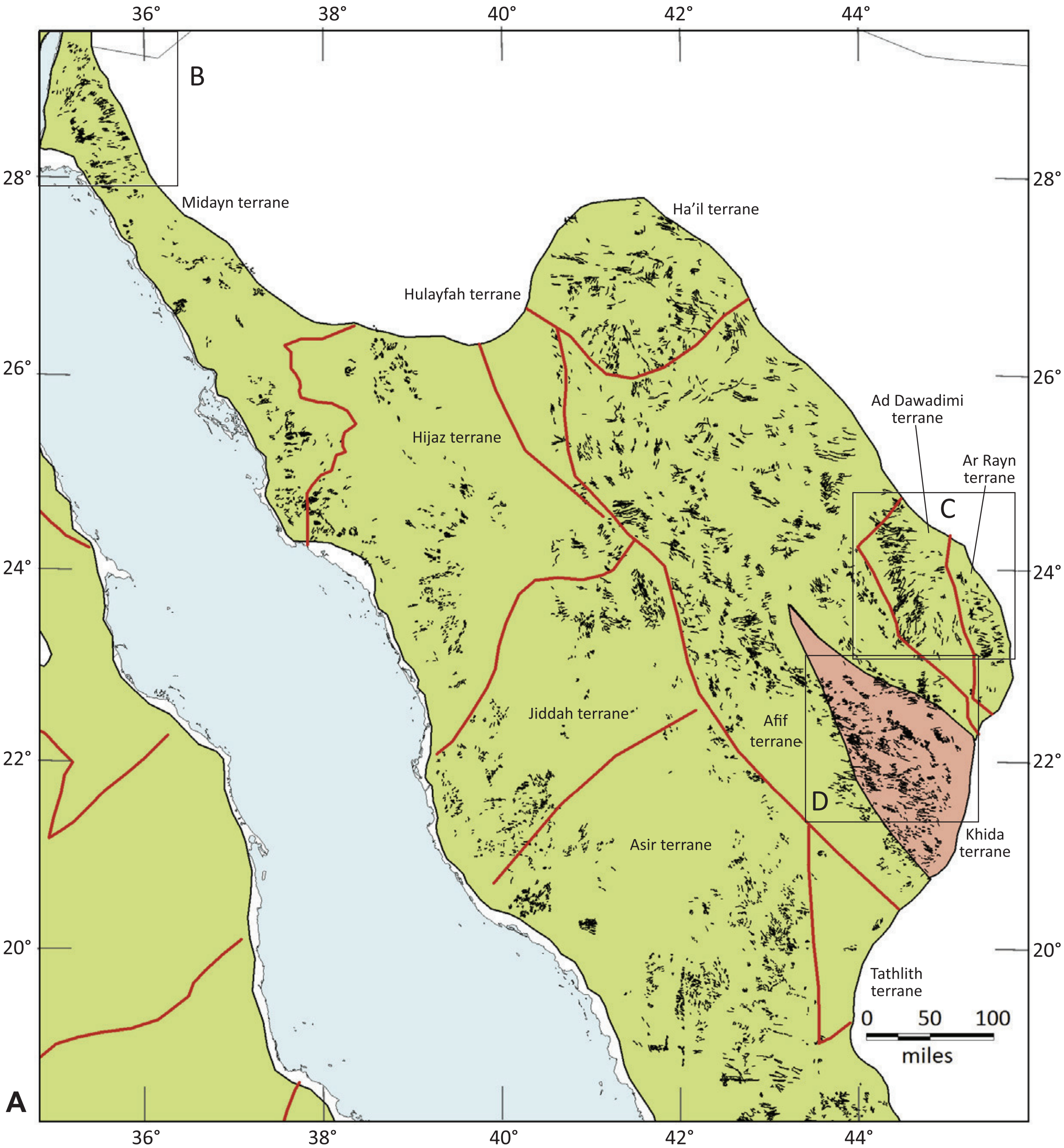

Fig. 25. Late Cryogenian–Ediacaran dikes swarms in the Arabian Shield. (A) A synoptic view showing the widespread distribution of dikes plotted on a simplified tectonic map of the shield. (B) Details of dikes in the Midyan terrane. Note the swing in orientation toward the Gulf of Aqaba reflecting rotation of Ediacaran dikes during Cenozoic sinistral strike slip on the Dead Sea transform. (C) Details of dikes in the Ad Dawadimi and Ar Rayn terranes. Note the change in prevailing dike orientation from north to south in the Ad Dawadimi terrane suggesting variation in the extension direction. (D) Detail of dikes in the Khida terrane and adjacent areas. Arrows shows schematic directions of extension implied by the prevalent strike-orientations of the dikes.

intrusion 10 km across composed of a pyroxenite–hornblendite core, an intermediate zone of diorite–gabbro, and an outer ring of syenite. Concordant lenses of titaniferous magnetite are present in the core ranging in thickness from a few centimeters to 3 m and as much as 50 m long. The *Wadi Kamal* complex, NW of Yanbu' al Bahr in the northwestern Arabian Shield, is an irregular body of norite, anorthosite, gabbro, and leucogabbro forming southern and northern lobes connected by a trail of scattered intrusions in surrounding schist and amphibolite. Gabbro and anorthosite predominate; norite forms an outer margin to the southern lobe. Samples of magnetite contain as much as 26% Ti and between 0.30% and 1.21% V_2O_5. A smaller body of dunite, amphibole-rich gabbro, and an ultramafic–mafic layered complex immediately S of the Kamal complex is a target for nickel and PGM mineralization. The concentrically zoned mafic–ultramafic *Akrarem* complex in the Eastern Desert contains Cu–Ni–PGE mineralization with net-textured and massive lenses of pyrrhotite, pentlandite, and chalcopyrite, as well as Cr-magnetite (Helmy and Mogessie, 2001). The ages of these intrusions, and their mineralizations, are not known, but they are undeformed massive plutons and, as suggested in Section 4.2, are likely to be late Cryogenian–Ediacaran.

9. Discussion

As schematically shown in Fig. 3, the final 100 million years of development of the Arabian–Nubian Shield is widely modeled in

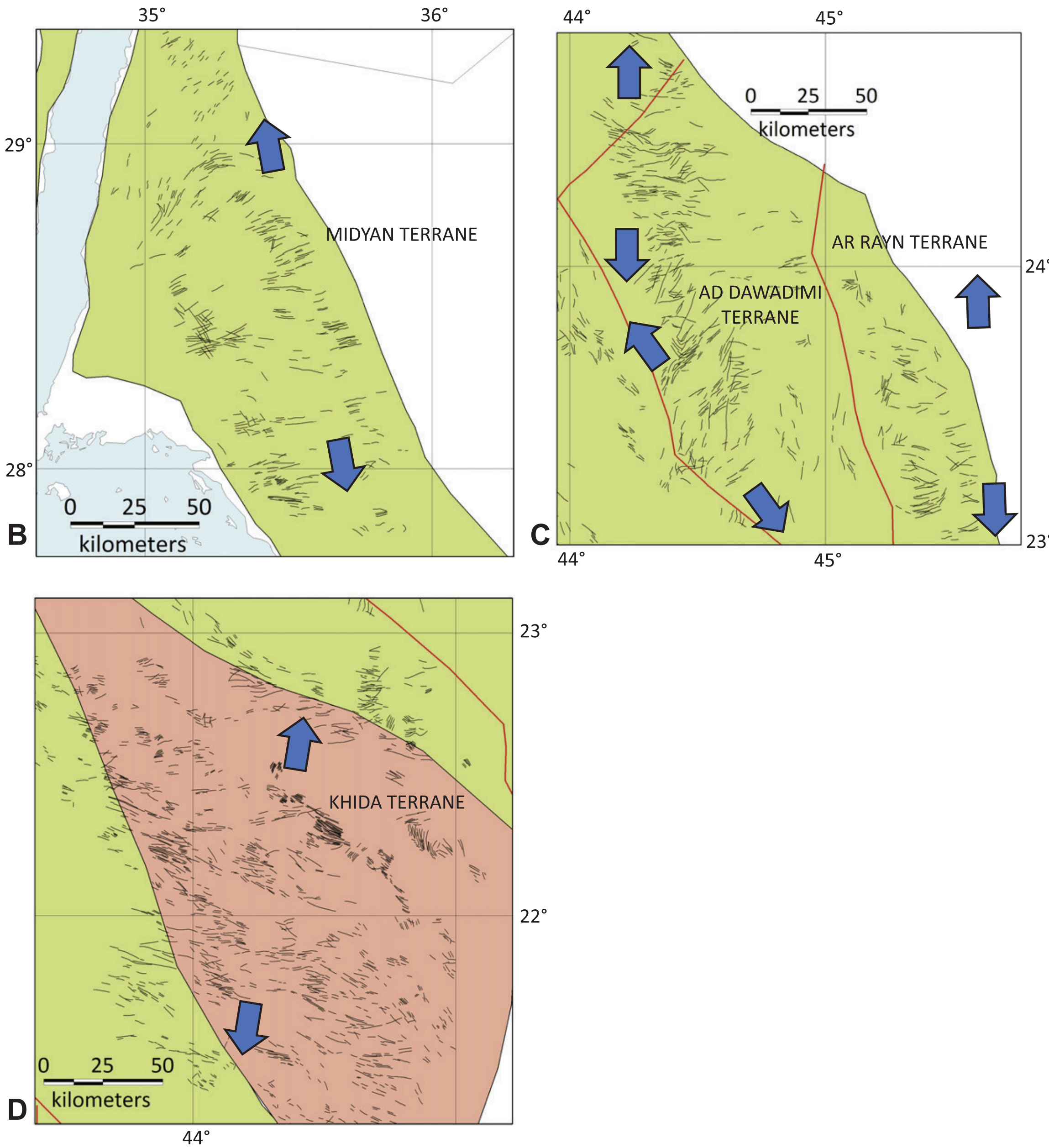

Fig. 25 (*continued*)

terms of crustal and lithospheric reworking. Elements in this process include transitions from peak orogeny to orogenic collapse, from lateral compression to pervasive lateral extension, from subduction-related magmatism and deposition to posttectonic/anorogenic magmatism and deposition, from the creation of intraoceanic juvenile arcs to the formation of a stable crust, and from periods of mountain-building and uplift to rapid and extensive erosional denudation.

Representative presentations of these transitions are by Stern (1994), Greiling et al. (1994), Abdeen and Greiling (2005), Blasband et al. (2000), Genna et al. (2002) and Johnson and Woldehaimanot (2003).

The model by Stern (1994), which is the background to the model shown in Fig. 3, and is widely accepted, initiates the formation of the ANS with seafloor spreading and the creation of arcs and backarcs following and during the breakup of Rodinia. Formation continued with the amalgamation of arc terranes and a few older continental fragments into new juvenile crust between about 870 Ma and 690 Ma. Continental collision and shortening first led to crustal thickening and uplift perhaps beginning about 750 Ma and continued with orogenic collapse and tectonic escape along strike-slip shear zones and faults until the end of the Precambrian.

The model of Greiling et al. (1994) and Abdeen and Greiling (2005) focuses on geologic events in the Eastern Desert of Egypt. They noted that the regional structure of the Eastern Desert mainly reflects post-collisional deformation characterized by extensional collapse, in some areas, and compression and (late) transpression, in other areas. Greiling and his colleagues noted the particular tectonostratigraphy of the Eastern Desert comprising suites of gneisses (Tier 1) structurally below low-grade supracrustal successions (Tier 2) (e.g., El Ramly, 1972; Bennet and Mosley, 1987; El-Gaby et al., 1988; Hermina et al., 1989; Shimron, 1990), but pointed out the lack of any difference between Tier 1 and Tier 2 rocks in terms of their protolith and geochemistry. They proposed that the two differ only in their degree of metamorphism and fabric and both represent juvenile Neoproterozoic crust, an interpretation unequivocally supported by geochronologic and isotopic research over the past three decades, for example by work on the Meatiq and Hafafit domes (Andresen et al., 2009; Liégeois and Stern, 2010). In the Greiling and Abdeen-Greiling model, early Neoproterozoic igneous and metamorphic terrane-forming events occurred between 900 and 600 Ma. Collisional deformation of the terranes ended about 615–600 Ma, marked by a transition from Cryogenian compressional tectonics associated with calc-alkaline magmatism to an Ediacaran tectonic style that was dominated by A-type alkali granite magmatism. Greiling et al. describe extensional collapse occurring between 595 and 575 Ma, generating features such as molasse basins, normal faults, uplifted metamorphic core complexes flanked by low-angle normal faults, and high-angle strike-slip shear zones. A distinctive feature of their model is that the post-collisional extensional phase associated with NNW–SSE compression, NW-folding, and SE-dipping thrusts, was followed by a short period of shortening, mainly in a NNW–SSE direction, which led to folding and thrusting toward the NNW, and a subsequent period of transpressional wrenching related to Najd faulting. The Najd faulting resulted in northwest-trending sinistral faults and positive flower structures with NE-verging folds and SW-dipping thrusts. Regional compression after extension is interpreted as a continuation of plate convergence after an episode of extensional collapse.

Blasband et al. (2000) emphasize the presence of a widespread phase of Ediacaran crustal extension at the end of development of the ANS, but do not envisage a subsequent phase of compression. Formation of the ANS began with an oceanic phase represented by ophiolites and island arcs, followed by arc accretion, the development of sutures, and lithospheric thickening. The terminal events, triggered by gravitational instability leading to collapse of the ANS orogen, included pervasive NW–SE extension contemporary with the development of metamorphic core complexes, late-orogenic extensional basins, and large strike-slip shear zones.

Genna et al. (2002), discussing the Arabian Shield, refer to pre-Panafrican structures (>690 Ma) and Panafrican structures (690–590 Ma) that overprint and partly obscure the earlier structures. The pre-Panafrican structures developed in association with the formation, amalgamation, and accretion of oceanic volcanosedimentary terranes and the emplacement of diorite to granitic intrusions. These precratonic units were brought together by collision at about 690 Ma, which closed the oceanic domain and created sutures. Subsequent Panafrican tectonism (690–590 Ma) is represented by a complex web of structures referred to as the Nabitah Belt comprising anastomosing strike-slip shear zones, gneiss domes, and foreland and intracontinental molasse basins. Genna et al. infer that subsequent widespread intracontinental extension (590–530 Ma) caused crustal thinning, bimodal magmatism, the emplacement of significant dike swarms, and volcanism. A marine transgression toward the end of the extension phase led to deposition of the Jibalah group and effectively ended formation of the Arabian Shield. Further shield history belongs to the Phanerozoic passive-margin that developed along the margin of the shield.

In the tectonic model of Johnson and Woldehaimanot (2003), the Arabian Shield is considered to consist of Archean and Paleoproterozoic continental crust at its margins and in the Khida terrane, and a large swath of Neoproterozoic (*c.* 870–670 Ma) continental–marginal and juvenile intraoceanic magmatic-arc terranes that accumulated in the Mozambique Ocean. Subduction began about 870 Ma, and initial arc–arc convergence and terrane suturing occurred at about 780 Ma, marking the beginning of ocean-basin closure and Gondwana assembly. Terrane amalgamation continued until about 600 Ma, resulting in the juxtaposition of eastern and western Gondwana. Terrane amalgamation was associated with overlapping periods of post-amalagamation basin formation, rifting, compression, strike-slip faulting, and the creation of gneiss domes in association with extension and/or thrusting. Final assembly of Gondwana was achieved by about 550 Ma. Most post-amalgamation basins contain molasse deposits, but those in the eastern Arabian Shield and Oman have marine to glaciomarine deposits, which indicate that seaways penetrated the orogen soon after orogeny. The varied character of the post-amalgamation events reflects alternating periods of Late Neoproterozoic extension and shortening, uplift and depression, deposition and erosion.

These models have many elements in common, but differ in detail about the timing and significance of the events that went into the creation of the ANS. It is worth considering, therefore, the evidence for some of the key elements in these models within the late Cryogenian–Ediacaran timeframe of this review.

9.1. Extension

A common theme in many Ediacaran tectonic models of the ANS is upper crustal extension both in a broadly N–S or NW–SE direction parallel to the orogen, and an E–W direction transverse to the orogen. The principal evidence for extension derives from a set of interrelated structural features: (1) dike swarms; (2) low-angle normal faults or detachments; and (3) transcurrent faulting and extensional basins.

9.1.1. Dike swarms

Late Cryogenian–Ediacaran mafic, felsic, and composite mafic–felsic dikes are widespread in the ANS. They are well known in the northern part of the Nubian Shield, Sinai, and Jordan (Stern et al., 1984; Abdel-Karim and El-Baroudy, 1995; Jarrar, 2001; Jarrar et al., 1992, 2004). Similar, although less well known, dike swarms are present in the Arabian Shield (Fig. 25) (Genna et al., 2002). Such dikes are unambiguous evidence of extension during the final stages of shield development (Stern et al., 1984; Stern, 1985; Genna et al., 2002). The dikes are posttectonic. They represent some of the youngest Neoproterozoic rocks in any given area and cross cut most other rocks and structures. Several of these dikes have been dated, including lamprophyre dikes that intrude the Ajjaj shear zone in the Midyan terrane (573 ± 6 Ma; Kennedy et al., 2011), a 577 ± 5 Ma dike that intrudes the Jibalah group in the north-central part of the Arabian shield (U–Pb zircon age; Kusky and Matsah, 2003), a 591 ± 9 composite dike from Feiran, Sinai (Stern and Manton, 1987), a 591 ± 12 Ma dike in NE Egypt (Stern and Voegeli, 1987), dikes between 600 and 540 Ma in northernmost Sinai (Kessel et al., 1998), pegmatite dikes between 574 ± 11 and 564 ± 10 Ma in Jordan (Jarrar et al., 1983), and composite and mafic dikes in Jordan dated at 575 ± 6 Ma and 545 ± 13 Ma (Jarrar, 2001). In detail, Genna et al. (2002) recognize multiple generations of posttectonic dikes. They occur in linear or curved swarms varying from a few centimeters to meters in thickness and from several meters to several tens of kilometers in length. In a given area, the dikes may have a common strike direction or form a conjugate system with intersecting strikes. The dikes are mostly subvertical, commonly rhyolitic, but include basalt and andesite. Bimodal swarms are common, containing andesitic and rhyolitic dikes that display intrusive relationships indicative of synchronous emplacement of mafic and felsic magma (Stern et al., 1984) or consist of composite dikes that individually are bimodal with felsic cores and mafic external parts (Jarrar et al., 2004; Stern and Voegeli, 1987; Katzir et al., 2007). The orientations of the swarms vary across the region and no systematic quantitative analysis of their strikes has been published other than work by Genna et al. (2002). But on inspection (e.g., Fig. 25; Fig. 2 in Stern et al., 1984; Fig. 1C in Jarrar et al., 1992), it is evident that the dikes in many swarms trend in an easterly direction. For example, those in the North and Central Eastern Desert trend NE (Stern et al., 1984;

Greiling et al., 1988, 1994) as do those in the Ha'il (Fig. 25A) and Midyan and Ar Rayn terranes in the Arabian Shield (Fig. 25B and C). Dikes in the Khida terrane trend ESE (Fig. 25D), whereas those in the Elat and Amran area (southern Israel) include older calc-alkaline N–S-trending dikes, younger tholeiitic NE–SW-trending dikes, and a few basalt dikes trending NW–SE (Kessel et al., 1998). The orientations of these dikes are strong evidence of broad northerly extension in the northern ANS during the Ediacaran. Garfunkel (1999) estimates that intrusion of swarms of basaltic to rhyolitic dikes in the northern ANS was accommodated by ~20 km regional dilation. It should be noted however, that not all easterly trending dikes in the Arabian–Nubian Shield are Ediacaran. Greiling et al. (1988) describe a major swarm of ENE-trending basaltic dikes in the northern part of the Hafafit dome that are intruded by the Gabal Abu Khrug ring complex (~90 Ma; Lutz et al., 1978) and are believed to be about 104 Ma (Greiling et al., 1988).

9.1.2. Low-angle normal faults and shear zones

Late Cryogenian–Ediacaran low-angle normal faults or detachments are reported from many parts of the ANS, likewise implying crustal extension. The most widely publicized are in the North and Central Eastern Desert and Sinai, described from gneiss domes and structural highs. The Meatiq and Hafafit domes are flanked on the north and south by NNW- and SSE-dipping normal faults, comprising post-accretion low-angle ductile shear zones with top to NNW or top to SSE senses of slip (Fritz et al., 1996, 2002; Fowler and Osman, 2009; Rice et al., 1992). In Sinai, Blasband et al. (1997, 2000) describe moderately NW-dipping shear zones with top-to-the-NW sense of shear in Wadi Kid, and conclude that this is an extensional core complex, although Fowler et al. (2010) suggest that the low-angle shears are collision-stage thrusts. U–Pb SHRIMP zircon ages reported by Stern et al. (2010a) constrain extension in the Kid complex to have occurred between ~600 MA and 585 Ma. The constraint is provided by a concordant age of 598 ± 8 Ma obtained from a rhyodacite clast in the Beyda Formation (Heib Formation of Shimron, 1984), which predates development of the Wadi Kid core complex, and a concordant age of 585 ± 8 Ma obtained from the Kid granite, which postdates the core complex. In the southern ANS, low-angle shear zones are reported from the ~100 km-long 1–5 km-wide north-trending Chulul shear zone in the Bilbul belt of Ethiopia, containing moderately east-dipping mylonitic fabric displaying a top-to-the-SE sense of movement (Tsige and Abdelsalam, 2005). Pervasive subhorizontal to moderately west-dipping foliations in HP–HT amphibolite-facies gneiss and schists occur in the Ghedem Domain in eastern Eritrea (Ghebreab, 1999). A low-angle, top-to-the-E/SE brittle–ductile shear zone separates the Ghedem Domain in the footwall from lower grade metavolcanic and metasedimentary rocks of the Nakfa or Bizen Domain in the hanging wall (Ghebreab and Talbot, 2000; Beyth et al., 2003). Overall, these structures suggest that NW–SE extension prevailed in the northern ANS, with extensional fabrics dipping NW and(or) SE, whereas E–W extension prevailed in the south.

9.1.3. Transcurrent faulting

As described above, late Cryogenian–Ediacaran transcurrent faults of the Najd system are conspicuous in the ANS. The faults are oblique to the main N–S trend of the EAO. In detail, the faults are transpressional structures with components of vertical as well as horizontal slip, but the prevailing sinistral sense of movement implies overall N–S extension parallel to the axis of the EAO. Additional evidence of extension in association with the Najd faults is the presence of the Dokhan–Hammamat and Jibalah group pull-apart basins located between left-stepping faults or in strain-releasing bends.

9.2. Exhumation, uplift, and denudation

Exhumation, uplift, and erosion are another set of interrelated processes widely modeled by many authors for the final 100 million years of evolution of the ANS. Exhumation refers to the return of once deep-seated metamorphic rocks to the Earth's surface and, particularly, refers to the unroofing of a rock defined by the vertical distance traversed relative to the Earth's surface (Ring et al., 1999). The term "uplift" has two aspects: one refers to the vertical motion of Earth's surface relative to sea level (surface uplift); the other to the vertical motion of rock relative to sea level (rock uplift). Denudation refers to the removal of material on the Earth's surface.

The process driving ANS exhumation is debated. One school of thought invokes orogenic collapse following the development of an ANS crust thickened by orogeny. Avigad and Gvirtzman (2009), for example, argue that extension and orogenic collapse in the northern ANS were associated with the removal and replacement of thickened lithospheric mantle by delamination. They estimate that mantle delamination would cause more than 3 km uplift. This would trigger rapid erosional unroofing of a rock carapace about 10 km thick and cause extension as well as decompression leading to partial melting of the ANS upper mantle and lower crust; perhaps this was responsible for the flood of posttectonic magmas? Erosional denudation may be followed by an episode of isostatic uplift but erosion, as well as thermal subsidence, would ultimately lower the surface to sea level. Other authors (e.g., Fritz et al., 1996) argue that no substantial crustal thickening occurred, at least in the Eastern Desert of Egypt, and infer that exhumation of, in this case, core-complex gneisses, was achieved as the result of enhanced heat flow along fault systems during oblique NW–SE transpression and by extension on normal faults. The enhanced heat flow would have enabled the formation of syn-extensional plutonism and triggered the exhumation of hot middle crust. Garfunkel (1999) infers that the northern ANS underwent rapid erosion beginning about 610 Ma following the magmatic phase at the end of the orogenic period, during which the upper 8–12 km of crust was removed in about 20 million years, lowering the average relief by about 2 km. Later, the area was differentiated into basins and highs associated with sedimentation and concurrent emplacement of high-level alkali-rich plutons, and was eroded, which further reduced the relief.

Direct evidence of exhumation, uplift, and denudation in the ANS includes: (1) regional angular unconformities and nonconformities and deposition of clastic sedimentary rocks; and (2) post-metamorphic and(or) post-intrusion mineral cooling ages testifying to tectonic exhumation.

9.2.1. Unconformities

Angular unconformities and nonconformities are present in the ANS at the base of post-amalgamation basins. It is not always certain when these unconformities developed but it is likely they developed due to uplift and denudation at many different times. The oldest unconformity considered in this review is the middle Cryogenian erosion surface that truncates the 660 ± 4 Ma Imdan plutonic complex at the base of the Thalbah group. The group itself was deposited in a terrestrial basin at some unknown elevation above sea level. Erosional truncation of the plutonic complex indicates several kilometers of exhumation prior to deposition of the Thalbah group, and the thick sequence of conglomerate, sandstone, and shale in the group itself evidences a vast amount of denudation.

The Murdama group in the northeastern ANS was deposited at or below sea level on an erosion surface truncating diorite, quartz diorite, tonalite, granodiorite, and gabbro of the Suwaj domain (~680 Ma) (Cole and Hedge, 1986) as well as mafic granulite (Cole, 1988). The presence of granulite beneath the Murdama unconformity implies as much as 15–20 km exhumation prior to Murdama deposition. The unconformity developed sometime between emplacement of the Suwaj domain and the onset of Murdama deposition, namely in the interval between 680 and 650 Ma. During the course of deposition, the basement of the Murdama group must have undergone at least 10–15 km subsidence so as to accommodate the thick clastic Murdama succession. The merely local presence of conglomerate in the Murdama and the relatively small conglomerate-clast size (pebble to cobble; not boulder) suggest little differential uplift at the margins of the Murdama basin, implying that erosion of the hinterland kept pace with exhumation. The thick succession of marine carbonates close to the base of the Murdama group demonstrates that the surface of the basin was at or below sea level. Murdama group deposition overlapped and followed the 680–640 Ma Nabitah orogeny yet the depositional environments of the basin and other marine post-amalgamation basins described earlier in this review, suggest that a large area in the ANS on either side of the Nabitah mobile belt lacked great elevation within a relatively short period after orogeny. Either denudation was intense or the Nabitah orogeny did not produce a high mountain range, perhaps because the area underwent shortening and extensive magmatism rather than a great degree of thrust stacking. In the Timna area, Israel, a cryptic unconformity developed sometime after emplacement of ~630 Ma dikes (Katz et al., 2004), which were metamorphosed at amphibolite facies, and after intrusion of the epizonal Timna granite ~610 Ma (Beyth et al., 1994).

In Egypt, the unconformities at the base of the Dokhan Volcanics and Hammamat Group developed sometime after emplacement and exhumation of 620–610 Ma granitoids. The coarse clastic sediments of the Hammamat Group are evidence that exhumation and erosion developed a land surface with significant relief, with conglomerates deposited at the discharges of high-relief drainage basins (Eliwa et al., 2010). The basins themselves have no marine sediments, indicating elevations in the western part of the ANS at this time above sea level. In Arabia, the minimum age of unconformities beneath the Jibalah group is not well constrained. Jibalah rocks in the Jifn basin, for example, overlie 625 Ma rhyolite (Kusky and Matsah, 2003), but in the Antaq basin overlie rocks of the Suwaj domain (~680 Ma). Differential uplift across basin margins is considered to be the cause of fanglomerates in some of the terrestrial dominated Jibalah basins (Kusky and Matsah, 2003). Stromatolitic carbonates and carbonates with indications of a marine isotopic signature in other Jibalah basins suggest that the northern and northeastern parts of the ANS had locally subsided below sea level by 580–560 Ma.

The most profound unconformity in the ANS is the vast erosion surface represented by the contact between the shield and overlying Lower Paleozoic sandstone (Fig. 26). Wherever observed, Lower Paleozoic sediments overlie a saprolitized-lateritic weathered profile a few meters thick passing down into less weathered shield rocks. The erosion surface has mostly low relief (Fig. 26) and the basal Paleozoic rock is sandstone with only scattered matrix-supported pebbles, not conglomerate. The sandstone was deposited by a continental-wide braided stream system with a constant south-to-north (present configuration) flow direction over a very gentle slope (Kolodner et al., 2006). The sandstone now has mostly been removed from the ANS but is preserved around the margins of and in rare outliers on the Arabian Shield. This sandstone probably covered most of the ANS at the time of its deposition. Intense chemical weathering is considered to be important for the formation of the sub-Paleozoic erosion surface (Avigad et al., 2005; Angerer et al., 2011). Subsequent Phanerozoic burial vertically compacted laterite to about 75% of its original thickness (Angerer et al., 2011). Worldwide, the Ediacaran was a period of glaciation, at ~630 (Marinoan) and ~580 Ma (Gaskiers) (Smith, 2009). Evidence for Ediacaran glaciation is reported from Oman (e.g., Brasier et al., 2000), but apart from local exposures of possible Jibalah-age diamictite, the presence of Ediacaran glaciers in the ANS remains to be demonstrated. It is therefore uncertain whether glaciation helped carve the end-Precambrian peneplain.

The sub-Paleozoic erosion surface locally truncates the Jibalah group and 580–560 Ma alkali granites, and in such localities the unconformity has a maximum age of about 560 Ma. Elsewhere, the erosion surface truncates much older rocks, and may reflect erosion considerably older than 560 Ma. Cole and Hedge (1986) infer that the northeastern Arabian Shield underwent as many as three major periods of erosion prior to deposition of Lower Paleozoic sandstone. Erosion between 640 and 615 Ma truncated the Murdama group and older rocks and formed the surface on which the Hibshi (632 Ma) and Jurdhawiyah (612–594 Ma) groups were deposited. Further erosion may have followed emplacement of diorite, granodiorite, and granite of the Idah suite (620–615 Ma). It is possible that emplacement of this suite, as well as the volcanic rocks of the Hibshi and Jurdhawiyah groups, resulted from such extensive partial melting that the density structure and isostatic equilibrium of the crust was altered enough to cause epeirogenic uplift, leading to renewed erosion and the production of local high-relief surfaces flanking Jibalah-group basins (Cole and Hedge, 1986). The Jibalah group and broadly contemporary peralkaline, peraluminous, and leucocratic granites of the Abanat suite (580–570 Ma) were, in turn, exhumed and eroded prior to deposition of the Lower Paleozoic sandstone cover. It is interesting to note that in several locations in the northeastern Arabian Shield, only the apical parts of Abanat suite plutons are exposed and rhyolitic flow and pyroclastic rocks vented by Abanat plutons are preserved, implying that the Abanat plutons and associated volcanic rocks were little exhumed and denuded. Idah suite plutons (~620; Cole and Hedge, 1986), in contrast, are eroded to deeper levels. Because little-eroded Abanat suite plutons and deeply eroded Idah suite plutons are exposed in adjacent outcrops, Cole and Hedge (1986) concluded that most erosion in the northeastern Arabian Shield occurred after emplacement of the Idah suite but before intrusion of the Abanat suite, likely, between about 615 and 580 Ma. Abanat suite plutons were intruded into crust that had already been exhumed and denuded, but were themselves little eroded prior to deposition of the Lower Paleozoic sandstone. Similar multiple periods of erosion are suggested for the northernmost ANS in Sinai, Negev, and Jordan (Samuel et al., 2007). The northern ANS contains A-type granitoids and ~580–530 Ma alkaline rhyolite and volcanic-equivalents such as the Dokhan Volcanics of Egypt and Feinan volcanic succession in Jordan. As in the northeastern Arabian Shield, the presence of late Ediacaran–Cambrian(?) intrusives and extrusive equivalents implies relatively little denudation and exhumation after their emplacement. But Samuel et al. (2007) infer that emplacement of the A-type rocks was preceded by a phase of extensive erosion associated with lithospheric extension and crustal rupture.

The Lower Paleozoic sandstone flanking the ANS represents a fluviatile environment that grades laterally and vertically in Jordan and Israel into a marine environment represented by the Burg limestone. At the end of the Precambrian, therefore, the surface of the ANS was mostly close to or above sea level, passing below sea level to the north and northeast (present-day coordinates) where continental crust of the newly formed EAO had a free ocean face. High mountains, however, existed farther S in EAO, part of the >8000-km-long and >1000-km-wide mountain chain (the Transgondwanan Supermountain) that formed following the oblique collision between eastern and western Gondwana (Squire et al., 2006) and provided much of the clastic material of the Lower Paleozoic sandstone.

9.2.2. Cooling ages

Although unconformities are important indicators of exhumation and denudation, the timing of exhumation is best determined by cooling ages. It is well known that faulting, among other processes, is capable of unroofing mid-crustal rocks. A hallmark of such unroofing is the resetting of footwall rocks to a common isotopic age reflecting cooling as the hangingwall is stripped away. As a consequence, low-temperature thermochronometry is a fundamental tool in identifying and dating exhumation (Stockli, 2005). The principle is that the age determined reflects cooling below the thermal blocking temperature of the rock or mineral being dated, rather than the age of mineral growth during metamorphism or the age of thermal resetting. In some cases, Rb–Sr and Sm–Nd whole-rock or mineral ages are interpreted as cooling ages (see examples in Appendix A). Most commonly, however, for the purposes of research in the ANS, cooling ages are determined by $^{40}Ar/^{30}Ar$ dating of hornblende, white mica, and sometimes feldspar. Rapid cooling, the hallmark of exhumation, is inferred if two minerals (commonly hornblende and white mica) extracted from the same sample have similar cooling ages, the argument being that for two minerals with different blocking temperatures to have the same age means that the host rock rapidly cooled and was therefore rapidly exhumed. The present Arabian–Nubian Shield $^{40}Ar/^{30}Ar$ age dataset includes 23 cooling ages (Table 1); other $^{40}Ar/^{30}Ar$ ages reflect thermal resetting or prograde metamorphism. The cooling ages spread between about 620 and 555 Ma with peaks at 575–580 Ma and 595–600 Ma (note that the ages shown in Fig. 27 designate the age at the beginning of each 5 million-year bin).

As indicated in Fig. 27, the main period of cooling and exhumation in the ANS was between 600 and 575 Ma. However, some variation occurs by region. Beyth et al. (2003) and Ghebreab et al. (2005) determined that crust in northeastern Ethiopia and eastern Eritrea underwent rapid exhumation between 640 and 545 Ma. Gneisses in the Ghedem domain in eastern Eritrea have average plateau ages of about 579 ± 6 Ma for hornblende and 567 ± 5 Ma for white mica (Ghebreab et al., 2005) (Table 1). The gneisses underwent peak metamorphism when *P–T* conditions were near 12 kbar and 650 °C at a depth of as much as 45 km. They subsequently rose to about 30 km and cooled at about 570 Ma, and further rose and cooled at about 567 Ma (Ghebreab et al., 2005). Exhumation was accomplished by extension on the low-angle shear surfaces described above (Beyth et al., 2003; Ghebreab et al., 2005). Final exhumation of Ethiopian and Eritrean crust occurred during the Cenozoic due to deformation (rift-margin uplift) related to the opening of the Red Sea. The same process of rift-margin uplift affected crustal rocks of the ANS in Yemen, Saudi Arabia, and Sinai. The crest of the Red Sea escarpment on both flanks of the southern Red Sea, in Eritrea–Ethiopia, Yemen, and southern Saudi Arabia is 2500–3000 m above sea level, and Cenozoic uplift of this amount must be taken into consideration when estimating end-Precambrian exhumation of ANS crustal rocks.

Basement rocks in northern Sinai were rapidly exhumed at about 600 Ma (Cosca et al., 1999). Peak regional metamorphism occurred in the mid-crust at about 620 Ma under *P–T* conditions of 7 ± 1 kbar (20–25 km depth) and 650–700 °C. Muscovite and biotite from the Elat schist, Taba gneiss, Elat granite, and Elat granitic gneiss record rapid exhumation and cooling at ~600 Ma, synchronous with widespread A-type igneous activity and a transition from orogenic to post-orogenic tectonics reflecting large-scale extension and tectonic escape (Cosca et al., 1999).

In the eastern Arabian Shield, rapid cooling is recorded by hornblende $^{40}Ar/^{30}Ar$ plateau ages of 612 ± 3, 611 ± 8, 610 ± 2, and 596 ± 6 Ma obtained from amphibolite and metagabbro in the Ar Ridaniyah ophiolite mélange in the central part of the Ad Dawadimi terrane. The ages reflect reactivation of the Ar Ridaniyah fault and rapid exhumation of the mélange (Al-Saleh and Boyle, 2001). To the south, a $^{40}Ar/^{39}Ar$ isochron age of 557 ± 15 Ma obtained from biotite paragneiss in the Kirsh gneiss along the Ar Rika fault zone is interpreted as the time of cooling below the biotite closure temperature (Al-Saleh, 2010). The age reflects exhumation of the gneiss and by implication, constrains the minimum age of development of the Kirsh gneiss dome.

Regional cooling and exhumation in the Egyptian Central Eastern Desert is constrained by Sm–Nd and Rb–Sr ages obtained from biotite, hornblende gneiss, and amphibolite in the core of the Hafafit dome (Abd El-Naby et al., 2008) and by $^{40}Ar/^{30}Ar$ hornblende and muscovite ages obtained from the Hafafit, Sibai, and Meatiq Domes (Fritz et al., 2002). The available data indicate that granite gneiss in the *Hafafit Dome* with protolith crystallization ages of 682 Ma (Stern and Hedge, 1985), 698 Ma and 700 Ma (Kröner et al., 1994), underwent amphibolite-facies metamorphism under conditions of 600–750 °C and 6–8 kbar. Peak metamorphism was attained at about 600 Ma or slightly earlier (Abd El-Naby et al., 2008). Cooling after this peak is indicated by garnet, plagioclase, and whole-rock Sm–Nd ages of 593 ± 4 Ma and 585 ± 8 Ma. A Rb–Sr biotite and whole-rock age of 573 ± 6 Ma obtained from biotite gneiss and $^{40}Ar/^{39}Ar$ hornblende plateau ages of 586 Ma and

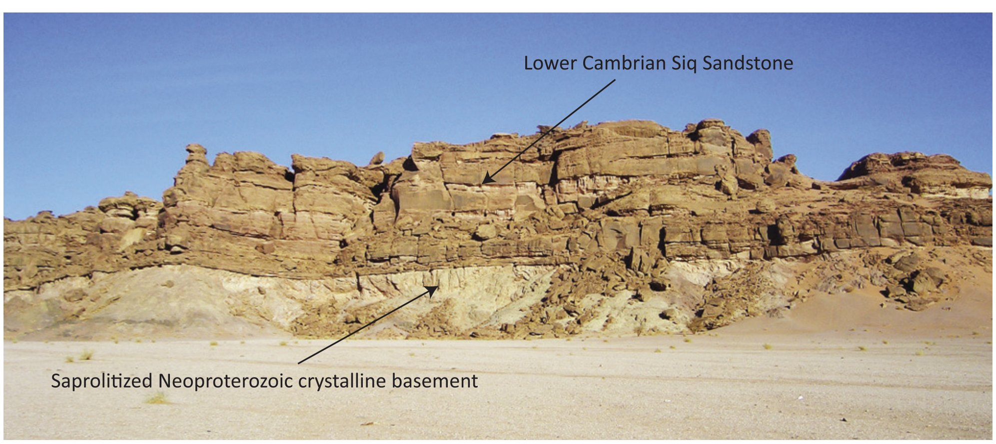

Fig. 26. Unconformity at the contact between the Arabian Shield and Lower Paleozoic sandstone, represented by a low-relief erosion surface exposed in a cliff about 50 m high about 25 km southwest of Al 'Ula at the northern margin of the shield in Saudi Arabia. At this locality, the shield rocks comprise Cryogenian greenstone and plutonic rocks belonging to the Midyan terrane. The Lower Paleozoic is sandstone and pebbly sandstone assigned to the Siq Sandstone. The shield rocks are deeply weathered for several meters beneath the unconformity, and present as saprolite.

584 Ma reflect further cooling and exhumation (Abd El-Naby et al., 2008) possibly localized along northeast-trending extensional faults (Fritz et al., 2002).

Hornblende $^{40}Ar/^{39}Ar$ plateau ages of 587 Ma, 583 Ma, 580 Ma, and 579 Ma from the Um Ba'anib gneiss indicates contemporary cooling and exhumation in the *Meatiq Dome*. Garnet-kyanite metapelite in the Meatiq Dome underwent peak metamorphism of ~750 °C and 8 kbar (about 27 km depth). This was followed by decompression to 4–5 kbar (13–17 km depth) (Neumayr et al., 1998) with a $^{40}Ar/^{39}Ar$ muscovite age suggesting rapid cooling and exhumation at about 583 Ma (Fritz et al., 2002). Muscovite from strike-slip and extension shear zones on the west and south of the Meatiq Dome yield plateau metamorphic ages of ~588 Ma and ~595 Ma indicating slip on the shear zones contemporary with 583 Ma exhumation within the dome (Fritz et al., 1996).

The *Sibai Dome*, in contrast, appears to have been exhumed 30 million years earlier at about 623 Ma with late cooling during exhumation and denudation after advective heating because of granite intrusion at 606 Ma (Fritz et al., 2002).

9.3. Orogenic collapse

It is common to refer to orogenic collapse in the closing stages of development of the ANS (Greiling et al., 1994; Fowler and El Kalioubi, 2004; Tsige and Abdelsalam, 2005; Ghebreab, 1999). Collapse occurs when lithostatic pressure exceeds rock strength limiting isostatically compensated elevation. The elevation of mountain belts (orogens) is determined by the balance between the force generated by plate convergence (collision), which causes the stacking of thrust sheets, buckling of rock sequences, crustal thickening, and the rise of mountains, and the force of gravity. With respect to the ANS, a pertinent question affecting the applicability of gravitational collapse concerns the amount by which the ANS was elevated above sea level at and after the peak of orogeny.

The *P–T* metamorphic conditions noted above suggest that a mountain belt existed in the southern ANS at about 650 Ma, and it is believed that this part of the ANS underwent rapid exhumation by orogenic collapse on low-angle shear zones between 640 and 545 Ma (Beyth et al., 2003). In contrast, the presence of marine post-amalgamation basins in the eastern ANS suggests that much of this part of the ANS was at or below sea level soon after the Nabitah orogeny peak deformation and metamorphism (680–640 Ma). The low elevations in the eastern ANS may reflect weak Ediacaran lithosphere due to largely molten lower crust (Stern and Johnson, 2010) but, whatever the cause, it is noteworthy that gravitational collapse has not been described from the eastern ANS.

Terrestrial Ediacaran deposits in the Eastern Desert and Sinai, conversely, suggest that the western ANS had greater elevation above sea level. It is therefore significant that published interpretations of gravitational collapse in the ANS are mostly reported from these areas. Fowler and El Kalioubi (2004), for example, describe the northwestward translation of intensely foliated ophiolite mélange and molasse deposits west of the Meatiq Dome as a gliding-spreading nappe caused by gravitational collapse following arc-collision and crustal thickening. Blasband et al. (2000) ascribe orogenic extension and collapse in the Wadi Kid area, Sinai, to gravitational instability created during the final stages of arc-accretion in the ANS.

A universal assumption of gravitational collapse in the ANS needs to be treated with caution however. Thus Fritz et al. (2002), discussing the same set of gneiss domes and molasse basins described by Fowler and El Kalioubi (2004) in terms of orogenic collapse, argue for exhumation of core complexes as the result of oblique island-arc collision zones associated with transpression and lateral extrusion. In this model, continuous magmatism weakened the crust and horizontal shortening was balanced by extension, creating a situation in which there was no major crustal thickening. It is envisaged that core complexes were continuously but slowly exhumed without creating significant relief, so there was no increase in potential energy and no gravitational collapse. In a similar vein, derivation of post-collisional magma from mantle sources is seen by Stern and Gottfried (1986) as indicating asthenosphere uplift and removal of upper mantle lithosphere, favoring orogenic extensional collapse (Dewey, 1988; Greiling et al., 1994).

9.4. Indentor and escape tectonics

Another topic commonly referred to in late Cryogenian–Ediacaran tectonic models for the ANS concerns orogenic collision or indentation and consequent lateral extrusion or tectonic escape. As described in Section 7.3 on the Najd fault system, the concept derives from work by Tapponnier and Molnar (1976) and Molnar and Tapponnier (1977) with regard to the indentation of Eurasia by the Indian craton and the creation of strike-slip faults in the Tibetan Plateau. The idea was subsequently discussed by Burke and Sengör (1986) who noted that buoyant continental or arc material in orogenic belts generally moves during collision along strike-slip shear zones toward a nearby oceanic margin or free face. The indentor concept was first applied to the Arabian Shield by Schmidt et al. (1979), who envisaged that the shield was indented from the east by a rigid block in eastern Arabia, which caused strike-slip deformation on the Najd fault system. Stern (1985) cautioned that predictions of the model with regard to specific structures in the ANS fail, but the concept has become a commonly accepted structural framework within which to analyze the

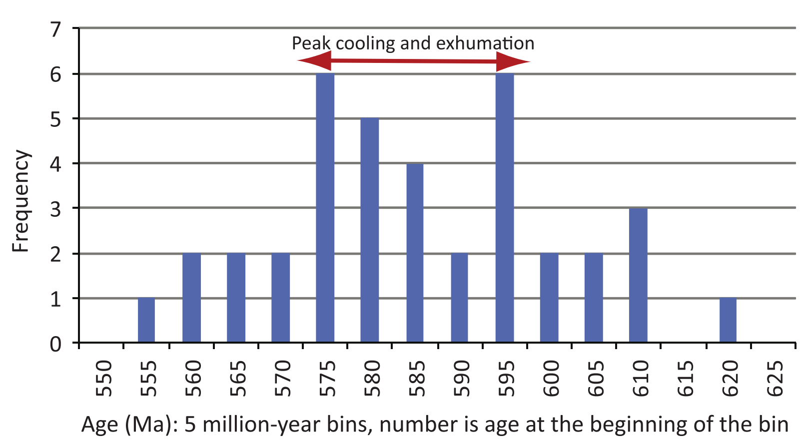

Fig. 27. $^{40}Ar/^{39}Ar$ cooling ages in the ANS. For sources of data, see Table 1.

processes of late Cryogenian–Ediacaran crustal shortening and orogen-parallel extension evident in the ANS. Berhe (1990) noted that northwest-trending strike-slip faults (i.e. the Najd system) exist throughout the ANS. It was inferred that they were the consequence of oblique collision although some of the kinematic assumptions were challenged by Abdelsalam and Stern (1991) in a discussion on the Berhe (1990) paper. In the context of the entire EAO, Bonavia and Chorowicz (1992) modeled the ANS as expelled northward from the Mozambique Belt because of indentation of East Africa by the Tanzanian craton. Jacobs and Thomas (2004) further developed this concept and proposed that indenter-escape tectonics on orogen parallel and orogen oblique shear zones occurred in both southern Africa and the ANS during collision of eastern and western Gondwana to form the East African–Antarctic Orogen. The existence of the East African–Antarctic Orogen as a continuous tectonic entity is disputed because East Africa and southern Africa are separated by an intervening E-trending orogenic belt (Hanson, 2003), and Collins and Pisarevsky (2005) pointed out that instead, the EAO appears to bifurcate south of Tanzania/Madagascar with one arm heading west into the Zambezi Belt and the other heading into India. However, the concept that ANS northward extrusion and southern African southward extrusion occurred during the final assembly of Gondwana is well grounded. A complication, of course, is that early models of the ANS being caught up in a hard collision between East and West Gondwana and extruding northward are simplistic because East Gondwana formed by a multiphase process of accretion and did not exist as a coherent single crustal block (Meert, 2002). Another complication is that not all orogen-parallel shear zones in the ANS necessarily reflect northward extension. Tsige and Abdelsalam (2005), for example, describe moderately E-dipping mylonitic zones in the ~100-km long north-trending Chulul shear zone in southern Ethiopia, the southern part of the Bulbul shear zone that have kinematic indicators showing top-to-the-SE tectonic transport. This sense of displacement is orthogonal to the trend of the EAO and is interpreted by Tsige and Abdelsalam (2005) in terms of easterly directed detachment and gravitation tectonic collapse rather than northward expulsion. The low-angle shear zones in Eritrea likewise reflect E–W gravity collapse between ~580–565 Ma rather than northward extension (Ghebreab, 1999; Ghebreab et al., 2005). Nonetheless, gross northward late Cryogenian–Ediacaran extension and, by implication, tectonic escape is inferred for the ANS on the basis of the sinistral sense of shear on the Keraf suture (Abdelsalam et al., 1998) indicating northward flow of the ANS relative to the Saharan Metacraton, the prevailing sinistral sense of shear on faults of the Najd fault system, and the widespread development of posttectonic dike swarms.

10. Gondwana assembly

Discussion about Gondwana assembly is not a prime objective of this review, and is more extensively covered in a pending companion review by Fritz and colleagues (this Journal). However, to contextualize our comments about indentor and escape tectonics, the development of the Abt formation and Al Amar arc, and the assembly of the ANS and its accretion to the Saharan Metacraton, we show a commonly accepted model of Gondwana assembly in Fig. 28 (Collins and Pisarevsky, 2005) and a cartoon of ANS assembly in Fig. 29, based on Fig. 28. The figures show that by 630 Ma, the core terranes of the ANS had already amalgamated forming the proto-Arabian–Nubian Shield (pANS), the Abt formation was being deposited on the flank of or close to the pANS, and the Al Amar arc was forming in what remained of the Mozambique Ocean. Marine and terrestrial post-amalgamation basins existed on the pANS, the region was being intruded by vast amounts of granitoids, and the pANS had begun to converge with the Saharan Metacraton. Between 620 and 580 Ma, the Al Amar arc and Abt formation accreted to the pANS, the pANS accreted with the Saharan Metacraton along the Keraf suture, and Ediacaran sedimentation ceased. Oblique collision resulting from convergence of Neoproterozoic India with the African parts of western Gondwana was focused in the southern part of the East African Orogen. This caused the development of orogen-parallel shear and shortening zones in the southern ANS, and transcurrent Najd faulting in the northern ANS, the general effect of which was northward tectonic escape. Exhumation of gneiss domes continued until ~580 Ma; granitoid magmatism continued until ~565 Ma. The crystalline basement of Eastern Arabia was in place by 540 Ma, prior to deposition of the lower Paleozoic sandstone that covered the entire region during the mid-Cambrian. Available evidence indicates that Eastern Arabia comprises juvenile Neoproterozoic rocks but as mentioned earlier in this review, the provenance of these rocks is uncertain—they may be an extension of the typical ANS or a separate crustal unit. We juxtapose it with the ANS in Fig. 29 at 620–550 Ma, and show the Al Amar arc, following Al-Husseini (2000), on the leading edge of the East Arabian crust, but we show its position at 630 Ma with a question mark because of the uncertainty of where Eastern Arabia formed in relation to the ANS.

11. Summary

We conclude this review by outlining, within the limits of available data, a chronology of Late Cryogenian–Ediacaran events in 10 million-year increments. We aim to highlight the fact that the end-Precambrian ANS continental crust was created by a large range of interacting depositional, magmatic, and structural events, and that any tectonic model for this period must account for contemporary subsidence, magma generation, shearing and shortening, exhumation, and erosion associated with the final amalgamation of the ANS terranes and collisional orogeny.

11.1. 650 Ma and earlier

By 650 Ma, most of the crust of the Arabian–Nubian Shield had formed, especially in the south. The western oceanic arc terranes had assembled along the Barka, Bi'r Umq–Nakasib, Yanbu–Sol Hamed–Allaqi–Heiani and Nabitah sutures, and had sutured with the Asir terrane along the Hulayfah–Ad Dafinah–Ruwah fault zone during the Nabitah orogeny (680–640 Ma). For convenience, we refer to this block of continental crust newly formed by terrane amalgamation as the proto-Arabian–Nubian Shield (pANS). Magmatism associated with the Nabitah orogeny was characterized by syntectonic gneisses emplaced along the Nabitah fault zone. The terrane assemblage existed east of, but not yet in contact with, the Saharan Metacraton (present coordinates), although oblique convergence between the two, along the eventual Keraf suture, was probably underway by 650 Ma. The northeastern margin of the pANS was marked by the Halaban ophiolite (emplaced ~680 Ma) and was flanked by an ocean basin. Active subduction in this oceanic basin was forming the Al Amar group (>689 Ma) and associated magmatic rocks (689–617 Ma) and oceanic sedimentation was forming the Abt formation, but the Abt formation and Al Amar arc did not accrete to the rest of the ANS for another 30 million years. Subduction beneath the pANS had probably largely ceased as a consequence of terrane amalgamation and suturing although some subduction, evidenced by continued convergence, shortening, and orogeny continued for another 100 million years during final assembly of the ANS. It is possible that delamination and sinking of detached subducted slabs, following peak orogeny, perturbed the mantle beneath the ANS crust facilitating the production of magmas and the phases of granitoid magmatism that characterized the remaining late Cryogenian–Ediacaran history of the ANS. Within the newly formed continental crust of the pANS, exhumation, uplift, and erosion followed by subsidence formed post-amalgamation depositional basins, the oldest of which, within the time frame of this review, comprised the terrestrial, intermontane Thalbah group (660–620 Ma).

11.2. 650–640 Ma

During this period, the northeastern part of the pANS was exhumed and eroded, revealing deep levels in the crust, and the crust subsequently subsided, forming post-amalgamation basins, which were filled by the Murdama group (650–625 Ma), in a foreland-type of basin, and Bani Ghayy group (∼650–620 Ma), in a fault-controlled (graben?) basin. These rocks were deposited on a profound regional unconformity that was developed across a large part of the northeastern ANS and accumulated in shallow-marine environments because of a late Cryogenian marine incursion. The Murdama and Bani Ghayy basins developed on the flank of and east of the Nabitah mobile belt; a small intermontane basin developed along the axis of the mobile belt in the south, filled by the Atura formation (<650 to >640 Ma). To the northwest, active terrestrial deposition continued in the Thalbah basin. In the 650–640 Ma period, furthermore, large parts of the eastern pANS (Arabian Shield) were intruded by calc-alkaline magma exemplified by suites of TTG and granite plutons such as the Laban complex (650 ± 7 Ma) in the Ha'il terrane, early phases of the Haml batholith, intrusions in the Siham arc (Jidh suite), and monzogranite–syenogranite plutons in the Asir terrane. Few plutonic rocks of this age are known in the Nubian shield. The plutons are largely undeformed and reflect the onset of posttectonic magmatism that characterized the remaining history of the pANS. Exceptions include a ∼649 Ma biotite granite in Ethiopia, a ∼647 Ma granite along the future Ar Rika shear zone, and a ∼640 Ma granite and diorite in Sinai that were subsequently deformed and converted into gneiss (Bielski, 1982; Kröner et al., 1990). Minor late syntectonic magmatism along the Nabitah fault zone marked the waning Nabitah orogeny (e.g., the Makhdhul quartz diorite gneiss 641 ± 3 Ma and the Tathlith gneiss 639 ± 6 Ma). This period witnessed the earliest orogenic gold mineralization in the ANS, with the formation of deposits at Ad Duwayhi (∼650 Ma). Deposition of the Abt formation and on-going arc-magmatism in the Ar Rayn terrane were active in the oceanic domain east of the pANS. Deformation, reflecting bulk E–W shortening, commenced on the north-trending Hamisana (660–550 Ma) and Oko (700–560 Ma) shear zones and fold belts in the southern ANS. Oblique sinistral convergence continued along the Keraf suture.

11.3. 640–630 Ma

This period was marked by continuing subduction in the oceanic basin east of the pANS, with a peak in TTG magmatism in the Al Amar arc, and by ongoing oblique convergence between the pANS and the Saharan Metacraton along the Keraf suture (Fig. 27). Metamorphism and deformation continued along shortening zones in the southern ANS. Marine environments persisted in post-amalgamation basins in the eastern ANS until about 625–620 Ma with continued deposition of the Murdama and Bani Ghayy groups. Folding and uplift of these deposits may have started soon after 630 Ma, resulting in a period of erosion that formed the regional unconformities on which the terrigenous and volcanic successions of the Hibshi, Hadn, and Jurdhawiyah units were subsequently deposited. The Hibshi formation (632 Ma) was probably deposited in a fault-controlled basin at the northern margin of the Murdama basin; the Hadn and Jurdhawiyah were deposited some 15 million years later. Marine connections were maintained in the heart of the pANS however, as evidenced by thick limestone in the Ablah group (640–615 Ma) of southern Arabia. Exhumation and brittle reactivation, forming small terrestrial molasse basins along the Nabitah fault zone, followed the emplacement of ∼640 Ma posttectonic granites. Voluminous calc-alkaline magmatism occurred in the northern and northeastern ANS (Aqaba complex 640–600 Ma and Marabit suite 635–580 Ma in the Midyan terrane; Khishaybi suite ∼640 Ma in the Afif terrane). Protoliths of the Um Ba'anib gneiss (631 ± 2 Ma) were emplaced in what would become the heart of the Meatiq Dome. The age of the Um Ba'anib gneiss constrains the maximum age of ductile deformation and the onset of northwesterly thrusting and tectonic transport in the Eastern Desert. This was broadly contemporary with the onset of shearing on the Qazaz–Ajjaj shear zone, evidenced by thermal resetting of the Raydan pluton (630 ± 19 Ma) and ductile deformation in the Thalbah group (<620 Ma). Orogenic gold mineralization continued, forming the An Najadi deposit in the Afif terrane (∼631 Ma), associated with the posttectonic calc-alkaline magmatism that was widespread in the northeastern Arabian Shield.

11.4. 630–620 Ma

Posttectonic A-type granites were emplaced in the ANS as early as the middle Cryogenian (Hamra and Bishah plutons, ∼686 Ma and ∼678 Ma), but the first major pulse of alkali magmatism occurred between 630 and 620 Ma, with the emplacement of plutons in the southern (Asir terrane) and northern (Afif and Midyan terranes) ANS. These granites marked the onset of highly fractionated intraplate, posttectonic magmatism and the beginning of a transition from convergent to extensional tectonics that characterized the remaining ANS history. The geographic spread of alkaline magma was limited, however, and there is no record of A-type magmatism at this time in the Eastern Desert or Sinai. Concurrent calc-alkaline magmatism in the Ar Rayn terrane reflected ongoing subduction in the oceanic domain east of the pANS. Within the pANS, subaerial volcanism occurred in the Shammar group (∼630–625 Ma), spatially associated with and the possible extrusive equivalents of alkali-feldspar granites. Deposition of the Murdama and Bani Ghayy groups in the marine post-amalgamation basins in the eastern ANS ceased during this period. Oblique convergence along the Keraf suture occurred, as did deformation on shortening zones in the southern ANS and transcurrent shearing began on the principal Najd faults in the northern ANS—the Halaban-Zarghat, Ar Rika, and Ruwah fault zones, indicating that transpressive E–W shortening and N–S orogen-parallel extension was pervasive in the pANS at this time. The Sibai gneiss dome was exhuming and cooling by about 623 Ma, reflecting the onset of Najd-related extension in the Eastern Desert; other gneiss domes in the Eastern Desert were exhumed in the following 30 million years.

11.5. 620–610 Ma

Significant posttectonic calc-alkaline magmatism continued during this period in parts of the Afif (Idah suite: 620–615 Ma), Asir, Midyan, and Hijaz terranes in the Arabian Shield, in Sinai, and in the Eastern Desert of Egypt. The Idah suite was associated with gold mineralization at Sukhaybarat (617 Ma). Magmatism was followed by exhumation and erosion, particularly in the northeastern Arabian Shield. Transcurrent slip on the Halaban-Zarghat and Ar Rika fault zones and the Qazaz and Ajjaj shear zones continued, as did transpressional sinistral convergence on the Keraf suture and deformation on shear zones and shortening zones in the southern ANS. Metamorphism of the Abt formation between 621 and 618 Ma (indicated by $^{40}Ar/^{39}Ar$ dating) is evidence of faulting and exhumation in parts of Abt basin. These events likely marked

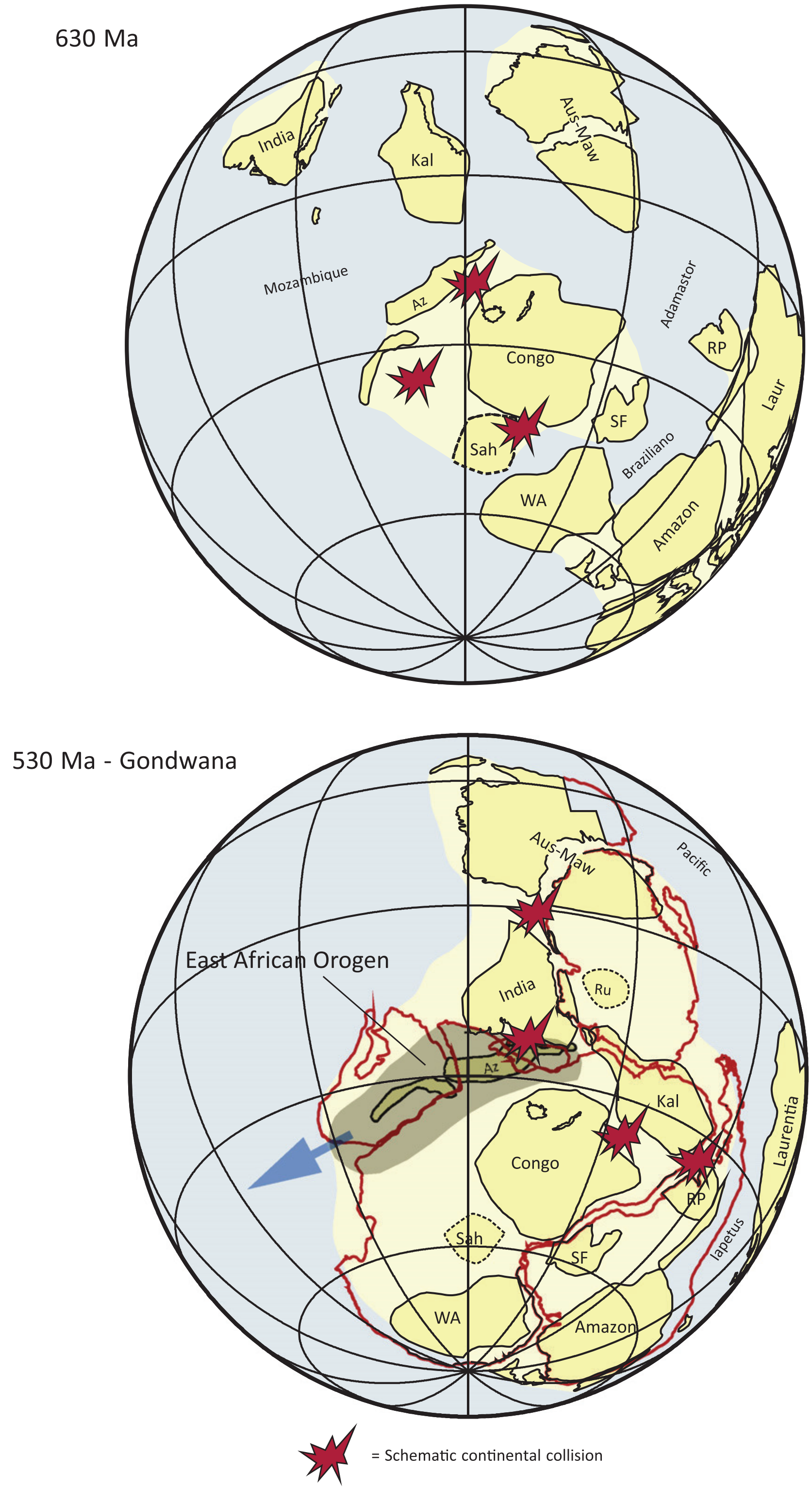

Fig. 28. Late Cryogenian–Ediacaran assembly of Gondwana, showing intense continent–continent collision between India and the Congo Craton in the East African part of the East African Orogen and the position of the Arabian–Nubian shield with an oceanic free face allowing tectonic escape (indicated by arrow). Modified from Collins and Pisarevsky (2005). Az = Azania; Kal = Kalahari craton; WA = West Africa; SF = Sao Francisco; Sah = Saharan Metacraton; RP = Rio de la Plata; Aus-Maw = Australia/Mawson block; Ru = Ruker Terrane.

the cessation of deposition in the basin, the onset of basin closure, and the beginning of the process that would eventually lead to the suturing of the Ad Dawadimi and Ar Rayn terranes and their amalgamation with the pANS. These tectonic events in the eastern ANS were contemporary with ongoing collision along the Keraf suture betweeen the ANS and Saharan Metacraton, and with tectonic escape in the core of the ANS. TTG calc-alkaline magmatism continued in the Al Amar arc until about 616 Ma, but following the

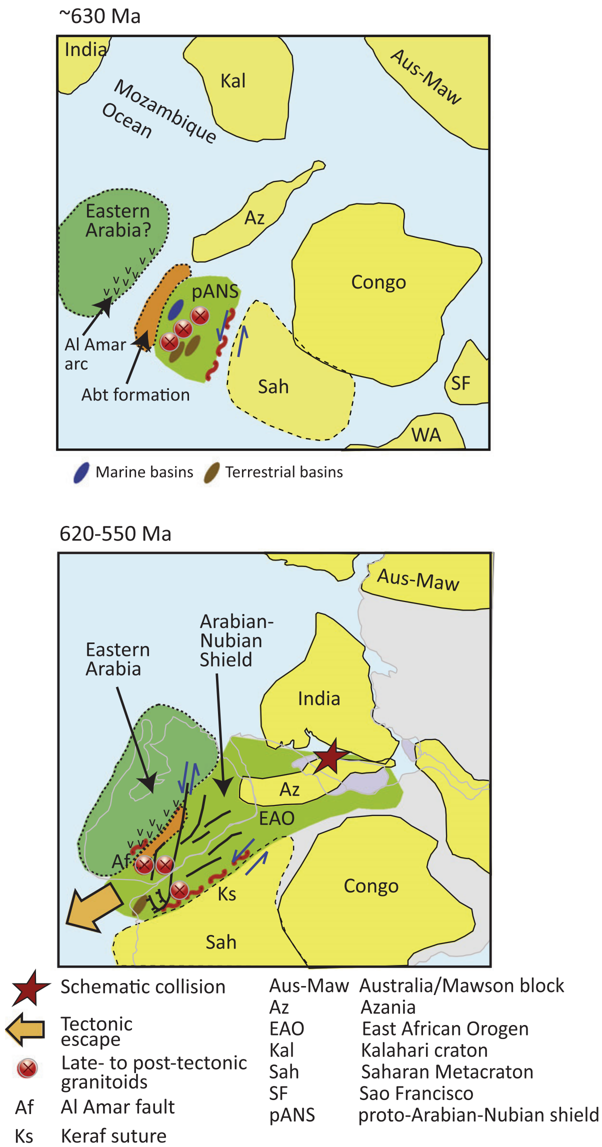

Fig. 29. Cartoon showing amalgamation and final accretion of the Arabian–Nubian Shield during the late Cryogenian and Ediacaran. Cartoon is based on the paleogeography illustrated in the Gondwana assembly model by Collins and Pisarevsky (2005) shown in Fig. 28.

waning or cessation of subduction beneath the arc, posttectonic alkali-feldspar granite magmatism became important. Intermontane molasse basins formed during this period in the western part of the pANS, filled by terrestrial sediments of the Hammamat Group and subaerial extrusives of the Dokhan Volcanics. The basins manifest extension and the formation of pull-aparts in a part of the ANS elevated above sea level and unaffected by marine influence. A major metamorphic event occurred in Sinai at about 620 Ma, followed 20 million years later by exhumation and cooling, further marking the transition from orogenic (compression) to post-orogenic (extension) tectonics.

11.6. 610–600 Ma

During this period, ductile deformation was active on the Qazaz, Halaban-Zarghat, Ar Rika, and Ruwah faults, concurrent with ongoing oblique convergence and orogen-parallel extension and tectonic escape throughout the pANS. At the same time, contact between the Saharan Metacraton and the pANS increased, with ongoing sinistral transpression on the Keraf suture. Thermal activity on the Hamisana and Oko shortening zones continued until ~550 Ma, indicating a persistence of E–W shortening, at least in the southern ANS, until virtually the end of the Precambrian. Further folding, low-grade metamorphism, and rapid exhumation and cooling in the Abt basin, recorded by $^{40}Ar/^{39}Ar$ ages of 616 Ma, 612, 611, and 610 Ma, and the onset of alkali-feldspar granite magmatism in the Al Amar arc (607–583 Ma) is believed to mark closure of the Abt marine basin and suturing between the Ad Dawdimi and Ar Rayn terranes. These events marked the elimination of the marine basin that had existed east of the earlier amalgamated pANS. Metamorphic rocks dating between 636 and 604 Ma, known from borehole intercepts east of the Ad Dawadimi and Ar Rayn terranes, in the basement of central Arabia (Al-Husseini, 2000, and references therein), were presumably also in place by this time but it is not clear whether the crust represents exotic material (part of eastern Gondwana?) or a continuation of juvenile Neoproterozoic material. Active deposition of Dokhan Volcanics and Hammamat Group rocks continued in terrestrial intermontane and molasse basins in western pANS and correlative terrestrial sedimentation and volcanism, represented by the Jurdhawiyah group (612–594 Ma), occurred at the eastern margin of the pANS. Further exhumation occurred in the Sibai gneiss dome and thrusting and ductile deformation occurred around the Meatiq Dome indicating major northwesterly tectonic transport at about 606 Ma. A different interpretation of the Abu Ziran diorite suggests significant extension. Voluminous posttectonic calc-alkaline magmatism occurred in much of the ANS, including Sinai (610–600), the Eastern Desert of Egypt, the Aswan area, Sabaloka, Ethiopia and Eritrea, and the Arabian Shield. A-type magmatism in Sinai and the Midyan and Eastern Desert terranes also occurred from about 608 Ma onward. The A-type magmatism, as well as evidence of rapid cooling and exhumation in Sinai at about 600 Ma, evidenced by $^{40}Ar/^{39}Ar$ dating, identifies pervasive post-collision extension and orogenic collapse in the northern ANS.

11.7. 600–590 Ma

A-type magmatism continued at this time in Sinai, the Central and Northern Eastern Desert, the Afif terrane, and Ar Rayn terrane. Concurrent calc-alkaline magmatism included the emplacement of monzogranite (~599 Ma) and monzodiorite (~598 Ma) in the Midyan terrane, hornblende–biotite granites (~599, 598 Ma) in the Saharan Metacraton; granites (~599–592 Ma) and quartz monzonite (~595 Ma) in Sinai; and granite and monzonite in the Sabaloka and Bayuda Desert area (~597, ~591 Ma). Bimodal alkali-calcic to alkali magmatism was represented by the Araba suite (~600–560 Ma), the result of melting of metasomatized mantle followed by shallow level feldspar-controlled fractionation in a rifting (extensional) environment. Emplacement of dike swarms constrained the cessation of metamorphism and ductile deformation and marked the onset of NW–SE directed extension in the northern ANS. Pre- to syntectonic granites with protolith ages of ~600 and ~597 Ma and a cooling age of ~600 Ma indicate the timing of peak metamorphism and deformation in the Atmur–Delgo terrane at the contact with the Saharan Metacraton and of major collision along the Keraf suture. Concurrent peak metamorphism at ~593 Ma occurred in Eritrea followed 15 million years later by exhumation and orogenic collapse. Ductile deformation and thrusting in the Meatiq Dome ceased by 590 Ma, constrained by emplacement of the posttectonic Arieki granite (590 Ma), concurrent with waning ductile deformation on Najd faults in the Arabian Shield. The Hafafit Dome underwent peak metamorphism at about 600 Ma or slightly earlier, followed by exhumation, cooling and extension between about 595 and 585 Ma. By ~590 Ma, ductile shearing on Najd faults in the Arabian Shield was ending; rapid exhumation and cooling occurred at the southern end of the Halaban-Zargaht fault between ~601 and ~597 Ma, and the Ruwah fault zone was intruded by posttectonic granite at about ~592 Ma. Active deposition continued in intermontane basins in the western ANS, however, with formation of Dokhan Volcanic rocks until at least ~592 Ma and deposition of Hammamat sediments until ~585 Ma. The Hammamat Goup in the type Hammamat basin was folded and overthrust by middle Cryogenian supracrustal rocks prior to the emplacement of the posttectonic Um Had granite at 596 Ma. The thrusting reflected bulk NE–SW shortening in the Eastern Desert. A transition to brittle deformation on several of the Najd faults marked the initiation of Jibalah group depositional basins at extensional zones along the faults.

11.8. 590–580 Ma

During this period, ductile deformation in the ANS was confined to Najd faults in the northwestern part of the Arabian Shield and perhaps in Egypt. The Meatiq Dome was exhuming and cooling, constrained by $^{40}Ar/^{39}Ar$ hornblende and white mica cooling ages of 587 Ma and 579 Ma obtained from the Um Ba'anib Orthogneiss. Exhumation affected the Hafafit Dome at about the same time with $^{40}Ar/^{39}Ar$ cooling ages between 593 Ma and 584 Ma following peak metamorphism. Slip on much of the Halaban-Zarghat fault had ceased by 588 Ma although deposition in extensional basins along the fault persisted and the Jibalah group continued to accumulate until about 565 Ma. Felsite emplaced at 587 Ma in already folded Abt formation confirms that the Abt basin was fully closed. Alkali-feldspar magmatism ceased in the Ar Rayn terrane but emplacement of strongly fractionated peralkaline, peraluminous, and related leucocratic granites continued at high levels in the crust elsewhere in the northeastern ANS and Sinai. Granites locally vented as rhyolitic flows and pyroclastic rocks.

11.9. 580–570 Ma

Ductile deformation and sinistral shearing occurred on the Qazaz–Ajjaj shear zones until 575 Ma, but ceased by 573 Ma, the age of posttectonic mafic dikes that intrude the shear zone. A final ductile deformation event on the Halaban-Zarghat fault zone is indicated by granite gneiss emplaced at 573 Ma, and alkali-feldspar granites intruded into the Abt formation denote a late Ediacaran phase of A-type magmatism (579–55 Ma) in the eastern ANS. Rapid exhumation and cooling on the Keraf suture (577 Ma) is taken as evidence that the pANS was almost fully accreted, at this time, to the Saharan Metacraton; which implies that assembly of the ANS was virtually complete. Rapid exhumation in Ghedem domain, Eritrea ($^{40}Ar/^{39}Ar$ ages ~579 and ~567 Ma) denotes ongoing orogenic collapse.

11.10. 570–560 Ma

During this period, Jibalah group deposition came to an end. Much of the group was deposited in terrestrial environments, but a late Ediacaran marine incursion is evidenced in the northern part of the ANS.

11.11. 560–550 Ma

Terminal exhumation on the Ar Rika fault, shown by $^{40}Ar/^{39}Ar$ cooling ages, occurred about 557 Ma, and orognic activity on the Keraf suture ceased by 560 Ma. Thus, by 560–550 Ma, orogeny in the ANS had ceased. The ANS thereafter underwent pervasive extension, as is indicated by the widespread emplacement of dike swarms until at least 545 Ma. By the end of the Ediacaran, the entire ANS had been subjected to strong chemical weathering and erosion, possibly in part effected by glaciation, and formed a vast low-relief erosion surface on which Lower Cambrian sandstone was eventually deposited.

Acknowledgments

The review represents a major international collaboration among authors whose work in the ANS spans three decades. The views expressed are based on an extensive body of literature, insights developed during prolonged periods of field work, and understanding gained from discussions with colleagues, but are ultimately those of the authors and are presented here as a summary of their present interpretations and a stimulus to further research. This review is a JEBEL contribution: R.J.S., A.A., and P.R.J. acknowledge the JEBEL Project as a means of bringing them together in the field, and providing a venue for gathering new information and exchanging ideas. Support for R.J.S. and P.R.J. to participate in the meeting was provided by NSF Grant 08221257. P.R.J. thanks Dr. Zohair Nawab, President, and colleagues at the Saudi Geological Survey for the opportunity to work on the Arabian Shield. A.A. acknowledges with thanks the staff and faculty at the Geology Department, Assiut University, particularly Dr. M.M.A. Abu El-Rus and Dr. E.M.S. El-Gaby, for exposing him to the geology, history, and problems of the Eastern Desert of Egypt. A.S.C's contribution forms TRaX Record #164. H.F. thanks the Austrian Science Foundation for financial support of a number of grants related to African geology (P12375, P09703, P15599, P12836, T247-N10) and colleagues at the Universities of Assuit and Mansour, Egypt. Funds for T.K. were provided by the National Natural Science Foundation of China (Grants 91014992 and 40821061) and the Ministry of Education of China (B07039). We thank Mohammed Abdelsalam and an anonymous reviewer for valuable comments that improved our final text, and acknowledge the Elsevier Press, the Journal of African Earth Sciences, and Tim Horscroft (editor) for the invitation to contribute this review.

Appendix A. Supplementary material

Supplementary data associated with this article can be found, in the online version, at doi:10.1016/j.jafrearsci.2011.07.003.

References

Abd El-Naby, H., Frisch, W., Siebel, W., 2008. Tectonic–metamorphic evolution of the Wadi Hafafit culmination (central Eastern Desert, Egypt). Implication for Neoproterozoic core complex exhumation in NE Africa. Geologica Acta 6, 293–312.

Abd El-Wahed, M.A., 2009. The role of the Najd fault system in the tectonic evolution of the Hammamat molasse sediments, Eastern Desert, Egypt. Arabian Journal of Geosciences. doi:10.1007/s12517-008-0030-0.

Abdalla, H.M., Mohamed, F.H., 1999. Mineralogical and geochemical investigation of emerald and beryl mineralisation, Pan-African Belt of Egypt: genetic and exploration aspects. Journal of African Earth Science 28, 581–598.

Abdeen, M.M., Abdelghaffar, A.A., 2011. Syn- and post-accretionary structures in the Neoproterozoic central Allaqi-Heiani suture zone, Southeastern Egypt. Precambrian Research 185, 95–108.

Abdeen, M.M., Greiling, R.O., 2005. A quantitative structural study of late Pan-African compressional deformation in the Central Eastern Desert (Egypt) during Gondwana assembly. Gondwana Research 8, 457–471.

Abdeen, M.M., Warr, L.N., 1998. Late orogenic basin evolution, deformation and metamorphism in the Pan-African Basement, Wadi Queih, Eastern Desert of Egypt. In: Naim, G.M., Hussein, A.A., Greiling, R.O., Warr, L.N. (Eds.), International Cooperation Scientific Series, 42, 272 pp.

Abdeen, M.M., Dardir, A.A., Greiling, R.O., 1992. Geological and structural evolution of the Wadi Queih Area (N Quseir), Pan-African basement of the Eastern Desert of Egypt. Zentralblatt fur Geologie und Palaeontolgie Teil I, 2653–2659.

Abdeen, M.M., Dardir, A.A., Greiling, R.O., 1997. Rain drop prints, mud crack polygons, and pebbles as strain markers in a Pan-African molasse basin, Wadi Queihm, Arabian Desert, Egypt. Annals of the Geological Survey of Egypt 20, 185–191.

Abdeen, M.M., Sadek, M.F., Greiling, R.O., 2008. Thrusting and multiple folding in the Neoproterozoic Pan-African basemenet of Wadi Hodein area, south Eastern Desert, Egypt. Journal of African Earth Sciences 52, 21–29.

Abdel-Karim, A.M., El-Baroudy, A.F., 1995. Petrology and geochemistry of felsic dyke swarms in SW Sinai, Egypt. Arab Gulf Journal of Scientific Research 13, 239–257.
Abdel-Monem, A.A., Radain, A.A., Gazzaz, M.A., 1982. Rb–Sr dating and petrology of Jabal Bitran granite, Idsas area, Saudi Arabia (abstract). Precambrian Research 16, A3.
Abdel-Rahman, A.M., Doig, R., 1987. The Rb–Sr geochronologic evolution of the Ras Gharib segment of the northern Nubian shield. Journal of the Geological Society, London 144, 577–586.
Abdelsalam, M.G., 1994. The Oko shear zone: post-accretionary deformations in the Arabian Nubian Shield. Journal of the Geological Society, London 151, 767–776.
Abdelsalam, M.G., Stern, R.J., 1991. Discussion of ophiolites in Northeast and East Africa: implications for Proterozoic crustal growth. Journal of the Geological Society, London 148, 602–604.
Abdelsalam, M.G., Stern, R.J., 1996. Sutures and shear zones in the Arabian–Nubian Shield. Journal of African Earth Sciences 23, 289–310.
Abdelsalam, M.G., Stern, R.J., Schandelmeier, H., Sultan, M., 1995. Deformation history of the Keraf Zone in NE Sudan, revealed by Shuttle Imaging Radar. Journal of Geology 103, 475–491.
Abdelsalam, M.G., Stern, R.J., Copeland, P., Elfaki, E.M., Elhur, B., Ibrahim, F.M., 1998. The Neoproterozoic Keraf suture in NE Sudan: Sinistral transpression along the eastern margin of West Gondwana. Journal of Geology 106, 133–147.
Abdelsalam, M.G., Liégeois, J.-P., Stern, R.J., 2002. The Saharan Metacraton. Journal of African Earth Sciences 34, 119–136.
Abdelsalam, M.G., Abdeen, M.M., Dowaidar, H.M., Stern, R.J., Abdelghaffar, A.A., 2003. Structural evolution of the Neoproterozoic western Allaqi–Heiani suture, southwestern Egypt. Precambrian Research 124, 87–104.
Abu-Alam, T.S., Stüwe, K., 2009. Exhumation during oblique transpression: the Feiran–Solaf region, Egypt. Journal of Metamorphic Geology 27, 439–459.
Agar, R.A., 1986. The Bani Ghayy group; sedimentation and volcanism in "pull-apart" grabens of the Najd strike-slip orogen, Saudi Arabian Shield. Precambrian Research 31, 259–274.
Agar, R.A., 1987. The Najd fault system revisited: a two-way strike-slip orogen in the Saudi Arabian Shield. Journal of Structural Geology 9, 41–48.
Agar, R.A., Stacey, J.S., Whitehouse, M.J., 1992. Evolution of the Southern Afif terrane – a Geochronologic Study. Saudi Arabian Deputy Ministry for Mineral Resources Open-File Report DGMR-OF-10–15, 41 p.
Akaad, M.K., Abu El Ela, A.M., 2002. Geology of the basement tocks in the eastern half of the belt between latitudes 25°30′ and 26°30′N Central Eastern Desert. Geological Survey of Egypt Paper 78, 118 p.
Akkad, M.K., El Ramly, M.F., 1958. Seven New Occurrence of the Igla Formation in the Eastern Desert of Egypt. Geol. Surv. Egypt, 37 p (Paper No. 3).
Akkad, M.K., Noweir, A.M., 1980. Geology and lithostratigraphy of the Arabian Desert orogenic belt of Egypt between latitudes 25°35′ and 26°30′N. King Abdulaziz University, Jiddah. Institute of Applied Geology Bulletin 3 (4), 127–134.
Akkad, M.K., El-Gaby, S., Abbas, A.A., 1967a. Geology and petrology of the migmatites around Feiran Oasis. Journal of Geology UAR 10, 67–87.
Akkad, M.K., El-Gaby, S., Abbas, A.A., 1967b. On the evolution of Feiran Migmatites, Sinai. Journal of Geology UAR 11, 49–58.
Albino, G.V., Jalal, S., Christensen, K., 1995. Neoproterozoic mesothermal gold mineralization at Sukhaybarat East mine. Transactions of the Institution of Mining and Metallurgy (Section B: Applied Earth Science) 104, B157–B170.
Al-Dabbagh, M.H., Dowd, P.A., 1996. Sukhaybarat Gold Mine, Saudi Arabia. Mineral Industry International, July 16–21.
Aldrich, L.T., 1978. Geochronologic Data for the Arabian Shield. Section l, Radiometric Age Determinations of Some Rocks from the Arabian Shield. Saudi Arabian Directorate General of Mineral Resources Project Report 240, pp. 1–9.
Aleinikoff, J.N., Stoeser, D.B., 1988. Zircon Morphology and U–Pb Geochronology of Seven Metaluminous and Peralkaline Post-orogenic Granite Complexes of the Arabian Shield, Kingdom of Saudi Arabia. Saudi Arabian Directorate General of Mineral Resources Open-File Report USGS-OF-06-5, 32 p.
Al-Husseini, M., 2000. Origin of the Arabian Plate Structures: Amar collision and Najd rift. GeoArabia 5, 527–542.
Ali, B.H., Wilde, S.A., Gabr, M.M.A., 2009. Granitoid evolution in Sinai, Egypt, based on precise SHRIMP U–Pb zircon geochronology. Gondwana Research 15, 38–48.
Al-Muallem, M.S., Smith, J.W., 1987. Geologic Map of the Ar Rawdah Quadrangle, Sheet 21F, Kingdom of Saudi Arabia. Saudi Arabian Deputy Ministry for Mineral Resources Geoscience Map GM-85, Scale 1:250,000, 25 p.
Al-Saleh, A.M., 2010. The Kirsh gneiss dome: an extensional metamorphic core complex from the SE Arabian Shield. Arabian Journal of Geosciences. doi:10.1007/s12517-0101-0179-1.
Al-Saleh, A.M., Boyle, A.P., 2001. Structural rejuvenation of the eastern Arabian shield during continental collision: $^{40}Ar/^{39}Ar$ evidence from the Ar Ridaniyah ophiolite mélange. Journal of African Earth Sciences 33, 135–141.
Al-Saleh, A.M., Boyle, A.P., Mussett, A.E., 1998. Metamorphism and $^{40}Ar/^{39}Ar$ dating of the Halaban ophiolite and associated units: evidence for two-stage orogenesis in the eastern Arabian shield. Journal of the Geological Society, London 155, 165–175.
Al-Shanti, A.M., 1976. Mineralization of Ad Dawadimi District, Kingdom of Saudi Arabia. Saudi Arabian Directorate General of Mineral Resources Bulletin 14, 50 p.
Al-Shanti, A.M., Gass, I.G., 1983. The upper Proterozoic ophiolite mélange zones of the easternmost Arabian Shield. Journal of the Geological Society, London 140, 867–876.
Al-Shanti, A.M.S., Mitchell, A.H.G., 1976. Late Precambrian subduction and collision in the Al Amar–Idsas region, Kingdom of Saudi Arabia. Tectonophysics 30, T41–T47.
Amer, R., Kusky, T.M., Ghulam, A., 2009. Lithological mapping in the Central Eastern Desert of Egypt using ASTER data. Journal of African Earth Sciences. doi:10.1016/j.jafrearsci.2009.06.004.
Amer, R.M., Kusky, T.M., Ghulam, A., 2010. New methods of processing ASTER data for lithological mapping. examples from Fawakhir, Central Eastern Desert of Egypt. Journal of African Earth Sciences 56, 75–82.
Anderson, J.L., 1983. Proterozoic anorogenic granite plutonism of N America. In: Medaris, L.G., Byers, C.W., Mickelson, D.M., Shanks, W.C. (Eds.), Proterozoic Geology, vol. 161. Geological Society of America Memoir, pp. 133–154.
Andersson, U.-B., Ghebreab, W., Teklay, M., Whitehouse, M.J., 2000. Ages and character of crust-forming and metamorphic events in east-central and northern Eritrea: new conventional and SIMS U–Pb and mineral P–T data. Journal of African Earth Sciences 30, 7.
Andre, C.G., 1989. Evidence for phanerozoic reactivation of the Najd fault system in AVHRR, TM, and SPOT images of Central Arabia. Photogrammetry Engineering and Remote Sensing 55, 1129–1136.
Andresen, A., Abu El-Rus, M.A., Myhre, P.I., Boghdady, G.Y., Corfu, F., 2009. U–Pb TIMS age constraints on the evolution of the Neoproterozoic Meatiq Gneiss Dome, Eastern Desert, Egypt. International Journal of Earth Sciences. doi:10.1007/s00531-007-0276.
Andresen, A., Augland, L.E., Boghdady, G.Y., Lundmark, A.M., Elnady, O.M., Hassan, M.A., 2010. Structural constraints on the evolution of the Meatiq gneiss domes (Egypt), East-African Orogen. Journal of African Earth Sciences 57, 413–422.
Angerer, T., Greiling, R.O., Avigad, D., 2011. Fabric development in a weathering profile at a basement-cover interface, the sub-Cambrian peneplain, Israel: implications for decollement tectonics. Journal of Structural Geology 33, 819–832.
Arslan, A.I., 1989. Contribution to the geochemistry of the El Sukari granite pluton, Eastern Desert, Egypt. In: Proceedings of the 1st Conference on Geochemistry, Alexandria University, Alexandria, Egypt. pp 1–18.
Augland, L.E., Andresen, A., Boghdady, G.Y., 2011. U–Pb ID-TIMS dating of igneous and metaigneous rocks from the El-Sibai area: time constrains on the tectonic evolution of the Central Eastern Desert, Egypt. International Journal of Earth Sciences. doi:10.1007/s00531-011-0653-3.
Avigad, D., Gvirtzman, Z., 2009. Late Neoproterozoic rise and fall of the northern Arabian–Nubian shield: the role of lithospheric mantle delamination and subsequent thermal subsidence. Tectonophysics. doi:10.1016/j.tecto.2009.04.018.
Avigad, D., Sandler, A., Kolodner, K., Stern, R.J., McWilliams, M., Miller, N., Beyth, M., 2005. Mass-production of Cambro–Ordovician quartz-rich sandstone as a consequence of chemical weathering of Pan-African terranes: environmental implications. Earth and Planetary Science Letters 240, 818–826. doi:10.1016/j.epsl.2005.09.021.
Avigad, D., Stern, R.J., Beyth, M., Miller, N., McWilliams, M.O., 2007. Detrital zircon U–Pb geochronology of Cryogenian diamictites and Lower Paleozoic sandstone in Ethiopia (Tigrai): age constraints on Neoproterozoic glaciation and crustal evolution of the southern Arabian–Nubian Shield. Precambrian Research 154, 88–106.
Bailo, T., Schandelmeier, H., Franz, G., Sun, C.-H., Stern, R.J., 2003. Plutonic and metamorphic rocks from the Keraf suture (NE Sudan). A glimpse of Neoproterozoic evolution on the NE margin of W. Gondwana. Precambrian Research 123, 67–80.
Bandel, K., Shinaq, R., 2003. Sediments of the Precambrian Wadi Abu Barqa Formation influenced by life and their relation to the Cambrian sandstones in southern Israel. Freiberger Forschungshefte C 499, 78–91.
Barker, F., Wones, D.R., Sharp, W.N., Desborough, G.Z., 1975. The Pikes Peak batholith, Colorado Front Range, and a model for the origin of the gabbro–anorthosite–syenite–potassic granite suite. Precambrian Research 2, 97–160.
Basahel, A.N., Bahafzalah, A., Omara, S., Jux, U., 1984. Early Cambrian carbonate platform of the Arabian shield. Neues Jahrbuch für Geologie und Paläontologie, Monatshefte (N. Jb., Geol. Paläont. Mh.), 113–128.
Bea, F., Abu-Anbar, M., Montero, P., Peres, P., Talavera, C., 2009. The 844 Ma Moneiga quartz-diorites of the Sinai, Egypt: Evidence for Andean-type arc or rift-related magmatism in the Arabian–Nubian shield? Precambrian Research 175, 161–168.
Be'eri-Shlevin, Y., Katzir, Y., Whitehouse, M.J., Kleinhanns, I.C., 2009a. Contribution of pre Pan-African crust to formation of the Arabian–Nubian Shield: New secondary ionization mass spectrometry U–Pb and O studies of zircon. Geology 37, 899–902.
Be'eri-Shlevin, Y., Katzir, Y., Whitehouse, M., 2009b. Post-collisional tectonomagmatic evolution in the northern Arabian–Nubian Shield: time constraints from ion-probe U–Pb dating of zircon. Journal of the Geological Society, London 166, 71–85.
Be'eri-Shlevin, Y., Katzir, Y., Valley, J.W., 2009c. Crustal evolution and recycling in a juvenile continent: oxygen isotope ratio of zircon in the northern Arabian Nubian Shield. Lithos 107, 169–184.
Be'eri-Shlevin, Y., Katzir, Y., Blichert-Toft, J., Kleinhanns, I.C., Whitehouse, M.J., 2010. Nd–Sr–Hf–O isotope provinciality in the northernmost Arabian–Nubian Shield: implications for crustal evolution. Contributions to Mineralogy and Petrology 160, 181–201.
Bennet, J.D., Mosley, P.N., 1987. Tiered-tectonics and evolution, E. Desert and Sinai, Egypt. In: Matheis, G., Schandelmerier, H. (Eds.), Current Research in African Earth Sciences. Balkema, Rotterdam, pp. 79–82.
Bentor, Y.K., 1985. The crustal evolution of the Arabo-Nubian massif with special reference to the Sinai Peninsula. Precambrian Research 28, 1–74.
Berhe, S.M., 1990. Ophiolites in NE and east Africa: implications for Proterozoic crustal growth. Journal of the Geological Society, London 147, 41–57.

Beyth, M., Stern, R.J., Altherr, R., Kröner, A., 1994. The late Precambrian Timna igneous complex, southern Israel: evidence for comagmatic-type sanukitoid monzodiorite and alkali granite magma. Lithos 31, 103–124.

Beyth, M., Avigad, D., Wetzel, H.-U., Matthews, A., Berhe, S.M., 2003. Crustal exhumation and indications for Snowball Earth in the East African Orogen, N Ethiopia and east Eritrea. Precambrian Research 123, 187–201.

Bielski, M., 1982. Stages in the Evolution of the Arabian–Nubian Massif in Sinai. Ph.D. Thesis, Jerusalem, Hebrew University, 155 p.

Billay, A.Y., Kisters, A.F.M., Meyer, F.M., Schneider, J., 1997. The geology of the Lega Dembi gold deposit, southern Ethiopia: implications for Pan-African gold exploration. Mineralium Deposita 32, 491–504.

Bingen, B., Jacobs, J., Viola, G., Henderson, I.H.C., Skar, Ø., Boyd, R., Thomas, R.J., Solli, A., Key, R.M., Daudi, E.X.F., 2009. Geochronology of the Precambrian crust in the Mozambique belt in NE Mozambique and implications for Gondwana assembly. Precambrian Research 170, 231–255.

Blasband, B., Brooijmans, P., Dirks, P., Visser, W., White, S., 1997. A Pan-African core complex in the Sinai, Egypt. Geologie en Mijnbouw 76, 247–266.

Blasband, B., White, S., Brooijmans, P., De Broorder, H., Visser, W., 2000. Late Proterozoic extensional collapse in the Arabian–Nubian Shield. Journal of the Geological Society, London 157, 615–628.

Boger, S.D., Miller, J.M., 2004. Terminal suturing of Gondwana and the onset of the Ross–Delamarian Orogeny: the cause and effect of an Early Cambrian reconfiguration of plate motions. Earth and Planetary Science Letters 219, 35–48.

Bonavia, F.F., Chorowicz, J., 1992. Northward expulsion of the Pan-African of NE Africa guided by a reentrant zone of the Tanzania craton. Geology 20, 1023–1026.

Bonin, B., 2007. A-type granites and related rocks. Evolution of a concept, problems, and prospects. Lithos 97, 1–29.

Botros, N.S., 2002. Metallogeny of gold in relation to the evolution of the Nubian shield in Egypt. Ore Geology Reviews 19, 137–164.

Brasier, M., McGarron, G., Tucker, R., Leather, J., Allen, P., Shields, G., 2000. New U–Pb zircon dates for the Neoproterozoic Ghubrah glaciation and the top of the Huqf Supergroup. Oman Geology 28, 175–178.

Bregar, M., 1996. Exhumation History of the Gebel Sibai Dome (Eastern Desert of Egypt): Constraints from Evolution of Low-angle Normal Faults and Corresponding Footwall Units. M.Sc. Thesis, University of Graz, Austria (unpublished).

Bregar, M., Bauernhofer, A., Pelz, K., Kloetzli, U., Fritz, H., Neumayr, P., 2002. A late Neoproterozoic magmatic core complex in the Eastern Desert of Egypt: emplacement of granitoids in a wrench-tectonic setting. Precambrian Research 118, 59–82.

Breitkreuz, C., Eliwa, H., Khalaf, I., El Gameel, K., Bühler, B., Sergeev, S., Larionov, A., Murata, M., 2010. Neoproterozoic SHRIMP U–Pb zircon ages of silica-rich Dokhan Volcanics in the northeastern Desert, Egypt. Precambrian Research 182, 163–174.

BRGM Geoscientists, 1993. Khnaiguiyah Zinc–Copper Deposit Prefeasibility Study: Synopsis of Geology and Mineralization: Saudi Arabian Directorate General of Mineral Resources Technical Report BRGM-TR-13-4.

Brito Neves, B.B.de., Cordani, U.G., 1991. Tectonic evolution of S America during the Late Proterozoic. Precambrian Research 53, 23–40.

Brown, G.B., 1972. Tectonic Map of the Arabian Peninsula. Saudi Arabian Directorate General of Mineral Resources Map AP-2, Scale 1:4,000,000.

Brown, G.F., Jackson, R.O., 1960. The Arabian Shield. XIX International Geological Congress, Pt. 9, pp. 69–77.

Brown, F.B., Schmidt, D.L., Huffman Jr., A.C., 1989. Geology of the Arabian Peninsula: Shield Area of Western Saudi Arabia. US Geological Survey Professional Paper 560-A, 188 p.

Burke, K., Sengör, C., 1986. Tectonic escape in the evolution of the continental crust. In: Barazangi, M., Brown, L. (Eds.), Reflection Seismology, vol. 14. American Geophysical Union Geodynamics Series, pp. 41–53.

Calvez, J.Y., Kemp, J., 1987. Rb–Sr geochronology of the Shammar Group in the Hulayfah Area, Northern Arabian Shield. Saudi Arabian Deputy Ministry for Mineral Resources Open-File Report BRGM-OF-07-11, 22 p.

Calvez, J.Y., Alsac, C., Delfour, J., Kemp, J., Pellaton, C., 1983. Geologic Evolution of Western, Central, and Eastern Parts of the Northern Precambrian Shield, Kingdom of Saudi Arabia. Saudi Arabian Deputy Ministry for Mineral Resources Open-File Report BRGM-OF-03-17, 57 p.

Calvez, J.Y., Alsac, C., Delfour, J., Kemp, J., Pellaton, C., 1984. Geological evolution of western, central, and eastern parts of the northern Precambrian Shield, Kingdom of Saudi Arabia. King Abdulaziz University, Jiddah, Faculty of Earth Science Bulletin 6, 24–48.

Calvez, J.Y., Delfour, J., Feybesse, J.L., 1985. 2000-million-years Old Inherited Zircons in Plutonic Rocks from the Al Amar Region. New Evidence for an Early Proterozoic Basement in the Eastern Saudi Arabian Shield? Saudi Arabian Deputy Ministry for Mineral Resources Open-File Report BRGM-OF-05-11, 27 p.

Cawood, P.A., Kroner, A., Collins, W.J., Kusky, T.M., Mooney, W.D., Windley, B.F., 2009.Accretionary Orogens through Earth History. Geological Society of London, Special Publication 2009, vol. 318, pp. 1–36. doi: 10.1144/SP318.1.

Church, W.R., 1991. Discussion of ophiolites in NE and East Africa: implications for Proterozoic crustal growth. Journal of the Geological Society, London 148, 600–601.

Cloud, P., Awramik, S.M., Morrison, K., Hadley, D.G., 1979. Earliest Phanerozoic or latest Proterozoic fossils from the Arabian Shield. Precambrian Research 10, 73–93.

Cole, J.C., 1988, Geology of the Aban al Ahmar Quadrangle, Sheet 25F, Kingdom of Saudi Arabia. Saudi Arabian Deputy Ministry for Mineral Resources Geoscience Map GM 105, Scale 1:250,000, 45 p.

Cole, J.C., Hedge, C.E., 1986. Geochronologic Investigation of Late Proterozoic Rocks in the Northeastern Shield of Saudi Arabia. Saudi Arabian Deputy Ministry for Mineral Resources Technical Record USGS-TR-05-5, 42 p.

Coleman, R.G., Brown, G.F., Keith, T.E.C., 1972, Layered Gabbros in SW Saudi Arabia. US Geological Survey Professional Papers 800-D, pp. D143–D150.

Collenette, P., Grainger, D.J., 1994. Mineral Resources of Saudi Arabia, not including Oil, Natural Gas, and Sulfur. Saudi Arabian Directorate General of Mineral Resources DGMR Special Publication SP-2, 322 p.

Collins, A.S., 2006. Madagascar and the Amalgamation of Central Gondwana. Gondwana Research 9, 3–16.

Collins, A.S., Pisarevsky, S.A., 2005. Amalgamating eastern Gondwana: the evolution of the Circum-Indian Orogens. Earth Science Reviews 71, 229–270.

Collins, A.S., Windley, B.F., 2002. The Tectonic Evolution of central and northern Madagascar and its place in the final assembly of Gondwana. Journal of Geology 110, 325–340.

Collins, W.J., Beams, S.D., White, A.J.R., Chappell, B.W., 1982. Nature and origin of A-type granites with particular reference to southeastern Australia. Contributions to Mineralogy and Petrology 80, 189–200.

Collins, A.S., Kinny, P.D., Razakamanana, T., 2010. Depositional age, provenance and metamorphic age of metasedimentary rocks from southern Madagascar. Gondwana Research. doi:10.1016/j.gr.2010.12.006.

Coolen, J.J.M.M.M., Priem, H.N.A., Verdurmen, E.A.T., Verschure, R.H., 1982. Possible zircon U-Pb evidence of Pan-African granuilite facies metamorphism in the Mozambique belt of southern Tanzania. Precambrian Research 17, 31–40.

Cooper, J.A., Stacey, J.S., Stoeser, D.B., Fleck, R.J., 1979. An evaluation of the zircon method of isotopic dating in the southern Arabian craton. Contributions to Mineralogy and Petrology 68, 429–439.

Cosca, M.A., Shimron, A., Caby, R., 1999. Late Precambrian metamorphism and cooling in the Arabian–Nubian Shield. Petrology and $^{40}Ar/^{39}Ar$ geochronology of metamorphic rocks of the Elat area (southern Israel). Precambrian Research 98, 107–127.

Cox, G., Lewis, C.J., Collins, A.S., Nettle, D., Halverson, G.P., Foden, J., Kattan, F., Jourdan, F., 2011. Ediacaran Terrane accretion in the Arabian Nubian Shield. Gondwana Research.

Creaser, R.A., Price, R.C., Wormald, R.J., 1991. A-type granites revisited: assessment of a residual source model. Geology 19, 163–166.

Darbyshire, D.P.F., Jackson, N.J., Ramsay, C.R., Roobol, M.J., 1983. Rb–Sr isotope study of latest Proterozoic volcano-sedimentary belts in the central Arabian Shield. Journal of the Geological Society, London 140, 203–213.

Dardir, A.A., Abu Zeid, K.M., 1972. Geology of the basement rocks between latitudes 27°00′ and 27°30′N, Eastern Desert. Annals of the Geological Survey of Egypt 2, 129–158.

Davies, F.B., 1984. Strain analysis of wrench faults and collision tectonics of the Arabian–Nubian Shield. Journal of Geology 82, 37–53.

Davies, F.B., 1985. Geological Map of the Al Wajh Quadrangle, Sheet 26B, Kingdom of Saudi Arabia. Saudi Arabian Deputy Ministry for Mineral Resources Geoscience Map GM 83, Scale 1:250,000, 27 p.

De Wall, H., Greiling, R.O., Sadek, M.F., 2001. Post-collisional shortening in the late Pan-African Hamisana high strain zone, SE Egypt: field and magnetic fabric evidence. Precambrian Research 107, 179–194.

Delfour, J., 1970. Le groupe de j'balah une nouvelle unite du bouchlier Arabe. Bureau de Recherches Géologiques et Minières Bulletin 2 (4), 19–32.

Delfour, J., 1977, Geology of the Nuqrah quadrangle, Sheet 25E, Kingdom of Saudi Arabia: Directorate General of Mineral Resources Geological Map GM 28, Scale 1:250,000, 32 p.

Delfour, J., 1982. Geologic Map of the Halaban quadrangle, Sheet 23G, Kingdom of Saudi Arabia. Directorate General of Mineral Resources Geologic Map GM 46, Scale 1:250,000, 32 p.

Dewey, J.F., 1988. Extensional collapse of orogens. Tectonics 7, 1123–1139.

Dodge, F.C.W., Helaby, A.M., 1974. Mineralization in the Uyaijah–Thaaban area, West Central Part of the Uyaijah Ring Structure, Kingdom of Saudi Arabia. US Geological Survey Saudi Arabian Project Report No. 191. 43 p.

Doebrich, J.L., Zahony, S.G., Leavitt, J.D., Portacio Jr., J.S., Siddiqui, A.A., Wooden, J.L., Fleck, R.J., Stein, H.J., 2004. Ad Duwayhi, Saudi Arabia. Geology and geochronology of a Neoproterozoic intrusion-related gold system in the Arabian shield. Economic Geology 99, 713–741.

Doebrich, J.L., Al-Jehani, A.M., Siddiqui, A.A., Hayes, T.S., Saleh, Y., Wooden, J.L., Johnson, P.R., Kattan, F.H., Shaikan, B., Basahel, M., Zahran, H., Al-Shammari, A., 2007. Geology and metallogeny of the Ara Rayn terrane, eastern Arabain shield. Evolution of a Neoproterozoic continental-margin arc during assembly of Gondwana within the East African Orogen. Precambrian Research 158, 17–50.

Drury, S.A., De Souza Filho, C.R., 1998. Neoproterozoic terrane assemblages in Eritrea: review and prospects. Journal of African Earth Science 27, 331–348.

Drysdall, A.R., Jackson, N.J., Ramsay, C.R., Douch, C.J., Hackett, D., 1984. Rare element mineralization related to Precambrian alkali granites in the Arabian shield. Economic Geology 79, 1369–1377.

du Bray, E.A., 1984. Geology of the Silsilah Ring Complex, Kingdom of Saudi Arabia. Saudi Arabian Deputy Ministry for Mineral Resources Technical Record USGS-TR-04-19, 78 p.

Duncan, I.J., Rivard, B., Arvidson, R.E., Sultan, M., 1990. Structural interpretation and tectonic evolution of a part of the Najd Shear Zone (Saudi Arabia) using Landsat thematic-mapper data. Tectonophysics 178, 309–315.

Duyverman, H.J., Harris, N.B.W., Hawkesworth, C.J., 1982. Crustal accretion in the Pan-African. Nd and Sr isotope evidence from the Arabian Shield. Earth and Planetary Science Letters 59, 315–326.
El Ramly, M.F., 1972. A New Geological Map for the Basement Rocks in the Eastern and Southwestern Deserts of Egypt. Annals of the Geological Survey, Egypt, scale 1:1,000,000, vol. 2, pp. 1–18.
El Ramly, M.F., Akaad, M.K., 1960. The Basement Complex in the Central-Eastern Desert of Egypt between Latitudes 24°30' and 25°40' N. Geological Survey of Egypt Paper 8, pp. 1–35.
El Ramly, M.F., Greiling, R., Kroner, A., Rashwan, A.A., 1984. On the tectonic evolution of the Wadi Hafafit area and environs, Eastern Desert of Egypt. King Abdulaziz University, Jiddah, Bulletin of the Faculty of Earth Sciences 6, 114–126.e.
El Ramly, M.F., Greiling, R.O., Rashwan, A.A., 1990. Comment on "Extension of the Najd shear system from Saudi Arabia to the Central Eastern Desert of Egypt based on integrated field and Landsat observations" by M. Sultan, R.E. Arvidson, I.J. Duncan, R.J. Stern, and B. El Kaliouby. Tectonics 9, 535–538.
El-Bialy, M.Z., 2010. On the Pan-African transition of the Arabian–Nubian Shield from compression to extension: the post-collision Dokhan volcanic suite of Kid-Malhak region, Sinai, Egypt. Gondwana Research 17, 26–43.
El-Gaby, S., El-Nady, O., Khudeir, A., 1984. Tectonic evolution of the basement complex in the Central Eastern Desert of Egypt. Geologische Rundshau 73, 1019–1036.
El-Gaby, S., Khudeir, A.A., El-Taky, M., 1989. The Sokhan Volcanics of Wadi Queih area, central Eastern Desert, Egypt. In: Proceedings of the 1st Conference on Geochemistry, Alexandria University, Egypt, pp. 42–62.
El-Gaby, S., List, F.K., Tehrani, R., 1988. Geology, evolution and metallogenesis of the Pan-African Belt in Egypt. In: El Gaby, S., Greiling, R. (Eds.), The Pan-African Belt of NE Africa and Adjacent Areas, Tectonic Evolution and Economic Aspects. Vieweg, Braunschweig, Wiesbaden, pp. 17–68.
El-Gaby, S., List, F.K., Tehrani, R., 1990. The basement complex of the Eastern Desert and Sinai. In: Said, R. (Ed.), The Geology of Egypt. Balkema, Rotterdam, pp. 175–184.
Eliwa, H.A., Abu El-Enen, M.M., Khalaf, I.M., Itaya, T., 2004. Metamorphic evolution of Sinai metapelites and gneisses: constraints from petrology and K/Ar dating. Egyptian Journal of Geology 48, 169–185.
Eliwa, H.A., Kimura, J.-I., Itaya, T., 2006. Late Neoproterozoic Dokhan Volcanics, N Eastern Desert, Egypt: Geochemistry and petrogenesis. Precambrian Research 151, 31–52.
Eliwa, H., Breitkreuz, C., Khalaf, I., El Gameel, K., 2010. Depositional styles of Early Ediacaran terrestrial volcanosedimentary succession in Gebel El Urf area, N Eastern Desert, Egypt. Journal of African Earth Sciences 57, 328–344.
El-Nisr, S.A., 1997. Late Precambrian volcanism at Wadi Allaqi, south Eastern Desert, Egypt: evidence for transitional continental arc/margin environment. Journal of African Earth Sciences 24, 301–313.
El-Rabaa, S.M., Al-Shumaimri, M.S., Al-Mishwat, A.T., 2001. Fate of the Najd fault system in northwestern Saudi Arabia and southwestern Jordan. Gondwana Research 4, 164–165.
Elsass, P, 1981. Geology and Mineralization of the Ar Ridaniyah Area. Saudi Arabian Deputy Ministry for Mineral Resources Open-File Report BRGM-OF-01-19, 39 p.
El-Shafei, M., Kusky, T.M., 2003. Structural and tectonic evolution of the Neoproterozoic Feiran–Solaf metamorphic belt, Sinai Peninsula. Implications for the closure of the Mozambique Ocean. In: Kusky, T., Abdelsalam, M., Tucker, R., Stern, R.J. (Eds.), Precambrian Research, Special Issue on The East African and Related Orogens, and the Assembly of Gondwana, pp. 269–293.
Fairer, G.M., 1985. Geological Map of the Wadi Baysh Quadrangle, Sheet 17F, Kingdom of Saudi Arabia. Saudi Arabian Deputy Ministry for Mineral Resources Geoscience Map GM-77, 1:250,000, 23 p.
Fike, D.A., Grotzinger, J.P., Pratt, L.M., Summons, R.E., 2006. Oxidation of the Ediacaran ocean. Nature 444, 744–747.
Finger, F., Dorr, W., Gerdes, A., Gharib, M., Dawoud, M., 2008. U–Pb zircon ages and geochemical data for the Monumental Granite and other granitoid rocks from Aswan, Egypt. Implications for geological evolution of the western margin of the Arabian–Nubian Shield. Mineralogy and Petrology 93, 153–183.
Fleck, R.J., Hadley, D.G., 1982. Ages and Strontium Initial Ratios of Plutonic Rocks in a Transect of the Arabian Shield. Saudi Arabian Deputy Ministry for Mineral Resources Open-File Report USGS-OF-03-38, 43 p.
Fleck, R.J., Greenwood, W.R., Hadley, D.G., Anderson, R.E., Schmidt, D.L., 1979. Rubidium–Strontium Geochronology and Plate-tectonic Evolution of the Southern Part of the Arabian Shield. US Geological Survey Saudi Arabian Mission Report 245, 105 p.
Fleck, R.J., Greenwood, W.R., Hadley, D.G., Anderson, R.E., Schmidt, D.L., 1980. Rubidium-Strontium Geochronology and Plate-tectonic Evolution of the Southern Part of the Arabian Shield. USGS Professional Paper 1131, 38 p.
Fowler, A., El Kalioubi, B., 2002. The Migif–Hafafit gneissic complex of the Egyptian Eastern Desert: fold interference patterns involving multiply deformed sheath folds. Tectonophysics 346, 247–275.
Fowler, A., El Kalioubi, B., 2004. Gravitational collapse origin of shear zones, foliations and linear structures in the Neoproterozoic cover nappes, Eastern Desert, Egypt. Journal of African Earth Sciences 38, 23–40.
Fowler, A., Hassen, I., 2008. Extensional tectonic origin of gneissosity and related structures of the Feiran–Solaf metamorphic belt. Precambrian Research 164, 119–136.
Fowler, T.J., Osman, A.F., 2001. Gneiss-cored interference dome associated with two phases of late Pan-African thrusting in the Central Eastern Desert, Egypt. Precambrian Research 108, 17–43.
Fowler, A., Osman, A.F., 2009. The Sha'it–Nugrus shear zone separating Central and S Eastern Deserts, Egypt: a post-arc collision low-angle normal ductile shear zone. Journal of African Earth Sciences 53, 16–32.
Fowler, A.-R., Khaled, G.A., Omar, S.M., Eliwa, H.A., 2006. The significance of gneissic rocks and synmagmatic extensional ductile shear zones of the Barud area for the tectonics of the North Eastern Desert, Egypt. Journal of African Earth Sciences 46, 201–220.
Fowler, A., Khamees, H., Dowidar, H., 2007. El Sibai gneissic complex, Central Eastern Desert, Egypt: folded nappes and syn-Kinematic gneissic granitoid sheets—note a core complex. Journal of African Earth Sciences 49, 119–135.
Fowler, A., Hassen, I.S., Osman, A.F., 2010. Neoproterozoic structural evolution of SE Sinai, Egypt: II. Convergent tectonic history of the continental arc Kid Group. Journal of African Earth Sciences 58, 526–546.
Fritz, H., Messner, M., 1999. Intramontane basin formation during oblique convergence in the Eastern Desert of Egypt: magmatically versus tectonically induced subsidence. Tectonophysics 315, 145–162.
Fritz, H., Puhl, J., 1997. Granitoid emplacement in a shear-extensional setting: A semiquantitative approach from physical parameters (Eastern Desert, Egypt). Zentralblatt fur Geologie und Palaeontolgie Teil 1, 257–276.
Fritz, H., Wallbrecher, E., Khudeir, A.A., Abu El Ela, F., Dallmeyer, D.R., 1996. Formation of Neoproterozoic metamorphic core complexes during oblique convergence (Eastern Desert, Egypt). Journal of African Earth Sciences 23, 311–329.
Fritz, H., Dallmeyer, D.R., Wallbrecher, E., Loizenbauer, J., Hoinkes, G., Neymayr, P., Khudeir, A.A., 2002. Neoproterozoic tectonothermal evolution of the Central Eastern Desert, Egypt: a slow velocity tectonic process of core complex exhumation. Journal of African Earth Sciences 34, 137–155.
Gabr, S., Ghulam, A., Kusky, T., 2010. Detecting areas of high-potential gold mineralization using ASTER data. Case study. Ore Deposit Reviews. doi:10.1016/j.oregeorev.2010.05.007.
Garfunkel, Z., 1999. History and paleogeography during the Pan-African orogen to stable platform transition: reappraisal of the evidence from the Elat area and the northern Arabian–Nubian Shield. Israeli Journal of Earth Science 48, 135–157.
Genna, A., Guerrot, C., Deschamps, Y., Nehlig, P., Shanti, M., 1999. Les formations Ablah d'Arabie Saoudite (datation et implication géologique). Compte Rendue Acadamie Sciences, Paris 329, 661–667.
Genna, A., Nehlig, P., Le Goff, E., Guetrrot, C., Shanti, M., 2002. Proterozoic tectonism of the Arabian Shield. Precambrian Research 117, 21–40.
Gettings, M.E., Blank, H.R., Mooney, W.D., 1986. Crustal structure of southwestern Saudi Arabia. Journal of Geophysical Research 91, 6491–6512.
Ghebreab, W., 1999. Tectono-metamorphic history of Neoproterozoic rocks in eastern Eritrea. Precambrian Research 98, 83–105.
Ghebreab, W., Talbot, C.J., 2000. Red Sea extension influenced by Pan-African tectonic grain in eastern Eritrea. Journal of Structural Geology 22, 931–946.
Ghebreab, W., Yohannes, E., Woldegiorgis, L., 1992. The Lega Dembi gold mine: an example of shear zone-hosted mineralization in the Adola greenstone belt. Journal of African Earth Sciences 15, 489–500.
Ghebreab, W., Talbot, C.J., Page, L., 2005. Time constrains on exhumation of the East African Orogen from field observations and $^{40}Ar/^{39}Ar$ cooling ages of low-angle mylonites in Eritrea, NE Africa. Precambrian Research 139, 20–41.
Ghebreab, W., Greiling, R., Solomon, S., 2009. Structural setting of Neoproterozoic mineralization, Asmara district, Eritrea. Journal of African Earth Sciences 55, 219–235.
Goldfarb, R.J., Groves, D.I., Gardoll, D., 2001. Orogenic gold and geologic time: a global synthesis. Ore Geology Reviews 18, 1–75.
Goldfarb, R.J., Baker, T., Dube, B., Groves, D.I., Hart, C.J.R., Gosselin, P., 2005. Distribution, Character, and Genesis of Gold Deposits in Metamorphic Terrains. Society of Economic Geologists, Inc., Economic Geology 100th Anniversary Volume, pp. 407–450.
Grainger, D.J., Hanif, M.R., 1989, Geologic Map of the Shaghab Quadrangle, Sheet 27B, Kingdom of Saudi Arabia. Saudi Arabian Directorate General of Mineral Resources Geologic Map GM 109, Scale 1:250,000, 31 p.
Greene, R.C., 1993. Stratigraphy of the Late Proterozoic Murdama group, Saudi Arabia. US Geological Survey Bulletin 1976, 59 p.
Greenwood, W.R., Anderson, R.E., Fleck, R.J., Roberts, R.J., 1980. Precambrian Geologic History and Plate Tectonic Evolution of the Arabian Shield. Saudi Arabian Directorate General of Mineral Resources Bulletin 24, 35 p.
Greenwood, W.R., Stoeser, D.B., Fleck, R.J., Stacey, J.S., 1982. Late Proterozoic Island-arc Complexes and Tectonic Belts in the Southern Part of the Arabian Shield, Kingdom of Saudi Arabia. Saudi Arabian Deputy Ministry for Mineral Resources Open-File Report USGS-OF-02-8, 46 p.
Greiling, R.O., 1997. Thrust tectonics in crystalline domains: the origin of a gneiss dome. Proceedings of the Indian Academy of Science (Earth and Planetary Sciences) 106, 209–220.
Greiling, R.O., Rashwan, A.A., 1994. Large-scale shear zones and related mineral deposits: examples from the Nubian Shield (Proterozoic), Egypt. Africa Geoscience Review 1, 503–514.
Greiling, R.O., Kröner, A., El Ramly, M.F., 1984. Structural interference patterns and their origin in the Pan-African basement of the southeastern desert of Egypt. In: Kröner, A., Greiling, R.O. (Eds.), Precambrian Tectonics Illustated. Schweizerbart'sche Verlagsbuchhandlung, Stuttgart, pp. 401–412.
Greiling, R.O., Kroner, A., EI Ramly, M.F., Rashwan, A.A., 1988a. Structural and geological relationship between the southern and central parts of the Eastern Desert of Egypt. In: EI-Gaby, S., Greiling, R.O., (Eds.), The Pan-African Belt of NE Africa and Adjacent Areas. Vieweg, Braunschweig, Wiesbaden, pp. 121–145.

Greiling, R.O., Abdeen, M.M., Dardir, A.A., El-Akhal, H., El-Ramly, M.F., Kamal El-Din, G.M., Osman, A.F., Rashwan, A.A., Rice, A.H.N., Sadek, M.F., 1994. A structural synthesis of the Proterozoic Arabian–Nubian Shield in Egypt. Geologische Rundshau 83, 484–501.
Greiling, R.O., Naim, G.M., Hussein, A.A., (Eds.), 1996. Excursion across the Pan-African, Neoproterozoic basement Qena–Quseir Guide Book. Centennial of the Egyptian Geological Survey 1896–1996. Egyptian Geological Survey and Mineral Authority, Cairo, Egypt.
Grothaus, B., Eppler, D., Ehrlish, R., 1979. Depositional environments and structural implications of the Hammamat Formation, Egypt. Annals of the Geological Survey of Egypt IX, 564–590.
Groves, D.I., Goldfarb, R.J., Gebre-Mariam, M., Hagemann, S.G., Robert, F., 1998. Orogenic gold deposits: a proposed classification in the context of their crustal distribution and relationship to other gold deposit types. Ore Geology Reviews 13, 7–27.
Grunow, A., 1999. Gondwana events and palaeogeography: a palaeomagnetic review. Journal of African Earth Sciences 28, 53–69.
Habib, M.E., Ahmed, A.A., El Nady, O.M., 1985. Tectonic evolution of the Meatiq infrastructure, Central Eastern Desert, Egypt. Tectonics 4, 613–627.
Hadley, D.G., 1974. The Taphrogeosynclinal Jubaylah Group in the Mashhad Area, Northwestern Hijaz, Kingdom of Saudi Arabia. Saudi Arabian Directorate General of Mineral Resource Bulletin 10, 18 p.
Halverson, G.P., Wade, B.P., Hurtgen, M.T., Barovich, K.M., 2010. Neoproterozoic chemostratigraphy. Precambrian Research 182, 337–350.
Hanson, R.E., 2003. Proterozoic geochronology and tectonic evolution of southern Africa. In: Yoshida, M., Windley, B.F., Dasgupta, S., (Eds.), Proterozoic East Gondwana: Supercontinent Assembly and Breakup: Geological Society, vol. 206. London, Special Publication, pp. 427–463.
Hargrove, U.S., 2006, Crustal Evolution of the Neoproterozoic Bi'r Umq Suture Zone, Kingdom of Saudi Arabia. Geochronological, Isotopic, and Geochemical Constraints. Unpublished Ph.D. Thesis, University of Texas at Dallas, 343 p.
Hargrove, U.S., Stern, R.J., Kimura, J.-I., Manton, W.I., Johnson, R., 2006. How juvenile is the Arabian–Nubian Shield? Evidence from Nd isotopes and pre-Neoproterozoic inherited zircon in the Bi'r Umq suture zone, Saudi Arabia. Earth and Planetary Science Letters 252, 308–326.
Harms, U., Darbyshire, D.P.F., Denkler, T., Hengst, M., Schandelmeier, H., 1994. Evolution of the Neoproterozoic Delgo Suture Zone and crustal growth in northern Sudan: geochemical and radiogenic isotope constrains. Geologische Rundschau 83, 591–603.
Hassan, M.A., Hashad, A.H., 1990. Precambrian of Egypt. In: Said, R. (Ed.), The Geology of Egypt. Balkema, Rotterdam, pp. 201–248.
Hedge, C.E., 1984. Precambrian Geochronology of Part of Northwestern Saudi Arabia. Saudi Arabian Deputy Ministry for Mineral Resources Open-File Report USGS-OF-04-31, 12 p.
Helmy, H.M., Mogessie, A., 2001. Gabbro Akarem, Eastern Desert, Egypt: Cu–Ni–PGE mineralization in a concentrically zoned mafic–ultramafic complex. Mineralium Deposita 36, 58–71.
Helmy, H.M., Kaindl, R., Fritz, H., 2004. The Sukari gold mine, Eastern Desert-Egypt: structural setting, mineralogy and fluid inclusion study. Mineralium Deposita 39, 495–511.
Hermina, M., Klitzsch, E., List, F.K., 1989. Stratigraphic Lexicon and Explanatory Notes to the Geological Map of Egypt. Conoco, Cairo, Scale 1:500,000.
Hoffman, P.F., Kaufman, A.J., Halverson, G.P., Schrag, D.P., 1998. A Neoproterozoic snowball Earth. Science 281, 1342–1346.
Hooper, P.R., Bailey, D.G., McCarley Holder, G.A., 1995. Tertiary calc-alkaline magmatism associated with lithospheric extension in the Pacific NW. Journal of Geophysical Research 100, 10303–10319.
Hume, W.F., 1934. Geology of Egypt – Part I – the Metamorphic Rocks. Government Press, Cairo.
Hurtgen, M.T., Halverson, G.P., Arthur, M.A., Hoffman, P.F., 2006. Sulfur cycling in the aftermath of a Neoproterozoic (Marinoan) snowball glaciation: evidence for a syn-glacial sulfidic deep ocean. Earth and Planetary Science Letters 245, 551–570.
Hussein, A.A., Ali, M.M., El Ramly, M.F., 1982. A proposed new classification of the granites of Egypt. Journal of Volcanology and Geothermal Research 14, 187–198.
Husseini, M.I., 1988. The Arabian Infracambrian extensional system. Tectonophysics 148, 93–103.
Jacobs, J., Thomas, R.J., 2004. Himalayan-type indenter-escape tectonics model for the southern part of the late Neoproterozoic–early Paleozoic East African orogen. Geology 32, 721–724.
Jarrar, G., 2001. The youngest Neoproterozoic mafic dyke suite in the Arabian shield. Mildly alkaline dolerites from S Jordan – their geochemistry and petrogenesis. Geological Magazine 138, 309–323.
Jarrar, G., Baumann, A., Wachendorf, H., 1983. Age determinations in the Precambrian basement of the Wadi Arab area, SW Jordan. Earth and Planetary Science Letters 63, 292–304.
Jarrar, G., Wachendorf, H., Saffarini, G., 1992. A late Proterozoic bimodal volcanic/subvolcanic suite from Wadi Araba, SW Jordan. Precambrian Research 56, 51–72.
Jarrar, G., Stern, R.J., Saffarini, G., Al-Zubi, H., 2003. Late- and post-orogenic Neoproterozoic intrusions of Jordan: Implications for crustal growth in the northernmost segment of the East African Orogen. Precambrian Research 123, 295–320.
Jarrar, G., Saffarini, G., Baumann, A., Wachendorf, H., 2004. Origin, age and petrogenesis of Neoproterozoic composite dikes from the Arabian–Nubian Shield, SW Jordan. Geological Journal 39, 157–178.
Jarrar, G.H., Manton, W.I., Stern, R.J., Zachmann, D., 2008. Late Neoproterozoic A-type granites in the northernmost Arabian–Nubian Shield formed by fractionation of basaltic melts. Chemie der Erde 68, 295–312.
Jelenc, D., 1966. Mineral Occurrences of Ethiopia. Ministry of Mines, Addis Ababa.720 p.
Johnson, P.R., 2003. Post-amalgamation basins of the NE Arabian Shield and implications for Neoproterozoic tectonism in the northern East African Orogen. Precambrian Research 123, 321–337.
Johnson, P.R., 2006. Explanatory Notes to the Map of Proterozoic Geology of Western Saudi Arabia. Saudi Geological Survey Technical Report SGS-TR-2006-4, 62 p., Scale 1:1,500,000.
Johnson, P.R., Kattan, F., 1999. The Ruwah, Ar Rika, and Halaban-Zarghat fault zones: NW-trending Neoproterozoic brittle–ductile shear zones in west-central Saudi Arabia, In: De Wall, H., Greiling, R.O. (Eds.), Aspects of Pan-African Tectonics, vol. 32. Bilateral Seminars of the International Bureau, Schriften des Forschungszentrum Jülich, pp. 75–79.
Johnson, P.R., Kattan, F., 2001. Oblique sinistral transpression in the Arabian shield: the timing and kinematics of a Neoproterozoic suture zone. Precambrian Research 107, 117–138.
Johnson, P.R., Kattan, F.H., 2007. Geochronologic Dataset for Precambrian Rocks in the Arabian Peninsula: a Catalogue of U–Pb, Rb–Sr, Ar–Ar, and Sm–Nd ages. Saudi Geological Survey Open-file Report SGS-OF-2007-3, 21 p.
Johnson, P.R., Stewart, I.C.F., 1995. Magnetically inferred basement structure in central Saudi Arabia. Tectonophysics 245, 37–52.
Johnson, P.R., Woldehaimanot, B., 2003. Development of the Arabian–Nubian shield: perspectives on accretion and deformation in the northern East African Orogen and the assembly of Gondwana. In: Yoshida, M., Windley, B.F., Dasgupta, S., (Eds.), Proterozoic East Gondwana: Supercontinent Assembly and Breakup: Geological Society, vol. 206. London, Special Publication, pp. 290–325.
Johnson, P.R., Kattan, F.H., Wooden, J.L., 2001. Implications of SHRIMP and microstructural data on the age and kinematics of shearing in the Asir Terrane, southern Arabian shield, Saudi Arabia. Gondwana Research 4, 172–173.
Johnson, P.R., Abdelsalam, M.G., Stern, R.J., 2003. The Bi'r Umq-Nakasib suture zone in the Arabian–Nubian Shield: a key to understanding crustal growth in the East African Orogen. Gondwana Research 6, 523–530.
Johnson, P.R., Kattan, F.K., Al-Saleh, A.M., 2004. Neoproterozoic ophiolites in the Arabian shield: field relations and structure. In: Kusky, T.M. (Ed.), Precambrian Ophiolites and Related rocks, Developments in Precambrian Geology, vol. 13. Elsevier, pp. 129–162.
Johnson, S.P., Rivers, T., De Waele, B., 2005. A review of the Mesoproterozoic to early Palaeozoic magmatic and tectonothermal history of South-central Africa: implications for Rodinia and Gondwana. Journal of the Geological Society, London 162, 433–450.
Kamilli, R.J., Cole, J.C., Elliott, J.E., Criss, R.E., 1993. Geology and genesis of the Baid al Jimalah tungsten deposit, Kingdom of Saudi Arabia. Economic Geology 88, 1743–1767.
Kattan, F.H., Harire, A.R., 2000. Geology of the Ad Duwayah-B'ir Warshah Mineral Belt: Saudi Geological Survey Open-File Report USGS-OF-99-6, 33 p.
Katz, O., Beyth, M., Miller, N., Stern, R., Avigad, D., Basu, A., Anbar, A., 2004. A Late Neoproterozoic (630 Ma) boninitic suite from southern Israel: Implications for the consolidation of Gondwanaland. Earth and Planetary Science Letters 218, 475–490.
Katzir, Y., Litvinovsky, B.A., Jahn, B.M., Eyal, M., Zanvilevich, A.N., Valley, J.W., Vapni, Ye., Beeri, Y., Spicuzza, M.J., 2007. Interrelations between coeval mafic and A-type silicic magmas from composite dykes in a bimodal suite of southern Israel, northernmost Arabian–Nubian Shield: Geochemical and isotope constraints. Lithos 97, 336–364.
Kellogg, K.S., Janjou, D., Minoux, L., Fourniguet, J., 1986. Geological Map of the Wadi Tathlith Quadrangle, Sheet 20G, Kingdom of Saudi Arabia. Saudi Arabian Deputy Ministry for Mineral Resources Geologic Map GM 103, Scale 1:250,000, 27 p.
Kemp, J., 1996. The Kuara Formation (northern Arabian shield); definition and interpretation: a probable fault-trough sedimentary succession. Journal of African Earth Sciences 22, 507–523.
Kemp, J., 1998. Caldera-related volcanic rocks in the Shammar Group, northern Arabian Shield. Journal of African Earth Sciences 26, 551–572.
Kemp, J., Pellaton, C., Calvez, J.Y., 1980. Geochronological Investigations and Geological History in the Precambrian of Northwestern Saudi Arabia. Saudi Arabian Directorate General of Mineral Resources Open-File Report BRGM-OF-01-1, 120 p.
Kennedy, A., Johnson, P.R., Kattan, F.H., 2004. SHRIMP Geochronology in the Northern Arabian Shield. Part I. Data Acquisition. Saudi Geological Survey Open-File Report SGS-OF-2004-11.
Kennedy, A., Johnson, P.R., Kattan, F.H., 2005. SHRIMP Geochronology in the Northern Arabian Shield. Part II. Data Acquisition 2004. Saudi Geological Survey Open-File Report SGS-OF-2005-10.
Kennedy, A., Kozdroj, W., Kattan, F.H., Kodzroj, M.Z., Johnson, P.R., 2010, SHRIMP Geochronology in the Arabian Shield (Midyan Terrane, Afif Terrane, Ad Dawadimi Terrane) and Nubian Shield (Central Eastern Desert), Part IV. Data Acquisition 2008. Saudi Geological Survey Open-File Report SGS-OF-2010-10, 101 p.
Kennedy, A., Kozdroj, W., Johnson, P.R., Kattan, F.H., 2011. SHRIMP Geochronology in the Northern Arabian Shield. Part III. Data Acquisition 2006. Saudi Geological Survey Open-File Report SGS-OF-2007-9.
Kessel, R., Stein, M., Navon, O., 1998. Petrogenesis of late Neoproterozoic dikes in the northern Arabian–Nubian Shield. Implications for the origin of A-type granites. Precambrian Research 92, 195–213.

Khudeir, A.A., Abu El-Rus, M.A., El-Gaby, S., El-Nady, O., Bishara, W.W., 2008. Sr–Nd isotopes and geochemistry of the infrastructural rocks in the Meatiq and Hafafit core complexes, Eastern Desert, Egypt: evidence for involvement of pre-Neoproterozoic crust in the growth of the Arabain–Nubian Shield. Island Arc 17, 90–108.

Klemm, D., Klemm, R., Murr, A., 2001. Gold of the Pharaohs – 6000 years of gold mining in Egypt and Nubia. Journal of African Earth Sciences 33, 643–659.

Kolodner, K., Avigad, D., McWilliams, M., Wooden, J.L., Weissbrod, T., Feinstein, S., 2006. Provenance of N Gondwana Cambrian–Ordovician sandstone: U–Pb SHRIMP dating of detrital zircons from Israel and Jordan. Geological Magazine 143, 367–391.

Kröner, A., Sassi, F.P., 1996. Evolution of the northern Somali basement: new constraints from zircon ages. Journal of African Earth Sciences 22, 1–15.

Kröner, A., Roobol, M.J., Ramsay, C.R., Jackson, N.J., 1979. Pan African ages of some gneissic rocks in the Saudi Arabian Shield. Journal of the Geological Society, London 136, 455–461.

Kröner, A., Greiling, R., Reischmann, T., Hussein, I.M., Stern, R.J., Durr, S., Kruger, J., Zimmer, M., 1987. Pan-African crustal evolution in the Nubian segment of NE Africa. In: Kröner, A. (Ed.), Proterozoic Lithospheric Evolution, American Geophysical Union Geodynamics Series, vol. 17, pp. 235–257.

Kröner, A., Eyal, M., Eyal, Y., 1990. Early Pan-African evolution of the basement around Elat, Israel, and the Sinai Peninsula revealed by single-zircon evaporation dating, and implications for crustal accretion rates. Geology 18, 545–548.

Kröner, A., Krüger, J., Rashwan, A.A.A., 1994. Age and tectonic setting of granitoid gneisses in the Eastern Desert of Egypt and south-west Sinai. Geologische Rundschau 83, 502–513.

Kusky, T.M., Matsah, M.I., 2000. Evolution of a Neoproterozoic Dextral Pull-apart Basin (Jifn Basin), NE Arabian Shield: Relationships to the Halaban-Zarghat (Najd) Fault System and the Closure of the Mozambique Ocean. Geological Society of America, Annual Meeting 2000.

Kusky, T., Matsah, M., 2003. Neoproterozoic Dextral Faulting on the Najd Fault System, Saudi Arabia, preceded sinistral faulting and escape tectonics related to closure of the Mozambique Ocean. In: Yoshida, M., Windley, B.F., Dasgupta, S., Powell, C. (Eds.), Proterozoic East Gondwana: Supercontinent Assembly and Breakup, vol. 206. Geological Society, London, Special Publication, pp. 327–361.

Kusky, T.M., Ramadan, T., 2002. Structural controls on Neoproterozoic mineralization in the SE Desert, Egypt. An integrated field, Landsat TM, and SIR C/X approach. Journal of African Earth Sciences 35, 107–121.

Kusky, T.M., Abdelsalam, M., Stern, R., Tucker, R., 2003. Preface to special issue on the East African and Related Orogens, and the Assembly of Gondwana. Precambrian Research 123, 81–85.

Küster, D., 2009. Granitoid-hosted Ta mineralization in the Arabian–Nubian Shield: ore deposit types, tectono-metallogenic setting and petrogenetic framework. Ore Geology Reviews 35, 68–86.

Küster, D., Liégeois, J.-P., 2001. Sr, Nd isotopes and geochemistry of the Bayuda Desert high-grade metamorphic basement (Sudan): an early Pan-African oceanic convergent margin, not the edge of the East Saharan ghost craton. Precambrian Research 109, 1–23.

Küster, D., Romer, R.L., Tolessa, D., Zerihun, D., Bheemalingeswara, K., 2007. Geochemical evolution and age of the Kenticha tantalum pegmatite, southern Ethiopia. In: International Symposium on Granitic Pegmatites: The State of the Art, May 2007, Porto, Portugal, Abstracts Volume, pp. 50–51.

Küster, D., Liégeois, J.P., Matukov, D., Sergeev, S., Lucassen, F., 2008. Zircon geochronology and Sr, Nd, Pb isotope geochemistry of granitoids from Bayuda Desert and Sabaloka (Sudan). Evidence for a Bayudian event (920–900 Ma) preceding the Pan-African orogenic cycle (860–590 Ma) at the eastern boundary of the Saharan Metacraton. Precambrian Research 164, 16–39.

Le Guerroué, L., Allen, P.A., Cozzi, A., 2006. Chemostratigraphic and sedimentological framework of the largest negative carbon isotopic excursion in Earth history: the Neoproterozoic Shuram Formation (Nafun Group, Oman). Precambrian Research 146, 68–92.

Lemiszki, P.J., Brown, L.D., 1988. Variable crustal structure of strike-slip fault zones as observed on deep seismic reflection profiles. Geological Society of America Bulletin 100, 665–676.

Lewis, C.J., 2009. A Structural, Geochronological and Geochemical Investigation of the Abt Schist; Ad Dawdimi Terrane, Central Saudi Arabia. University of Adelaide, Tectonics, Resources and Exploration, 88 p.

Lewis, R.S., Schull, H.W., 1994. Geology and gold mineralization of the An Najadi mineral belt and comparison to the Sukhaybarat gold mine, Kingdom of Saudi Arabia. Saudi Arabian Deputy Ministry for Mineral Resources Technical Report USGS-TR-94-6, 54 p.

Li, Z.X., Powell, C.M., 1993. Late Proterozoic to early Paleozoic paleomagnetism and the formation of Gondwanaland. In: Findlay, R.H., Unrug, R., Banks, M.R., Veevers, J.J. (Eds.), Gondwana Eight. Balkema, Rotterdam, pp. 9–21.

Li, Z.X., Bogdanova, S.V., Collins, A.S., Davidson, A., De Waele, B., Ernst, R.E., Fitzsimons, I.C.W., Fuck, R.A., Gladkochub, D.P., Jacobs, J., Karlstrom, K.E., Lu, S., Natapov, L.M., Pease, V., Pisarevsky, S.A., Thrane, K., Vernikovsky, V., 2007. Assembly, configuration, and break-up history of Rodinia: a synthesis. Precambrian Research 160, 179–210.

Liégeois, J.-P., Stern, R.J., 2010. Sr–Nd isotopes and geochemistry of granite–gneiss complexes from the Meatiq and Hafafit domes, Eastern Desert, Egypt: no evidence for pre-Neoproterozoic crust. Journal of African Earth Sciences 57, 31–40.

Liégois, J.-P., Navez, J., Hertogen, J., Black, R., 1998. Contrasting origin of post-collisional high-K calc-alkaline and shoshonotic versus alkaline and peralkaline granitoids. The use of sliding normalization. Lithos 45, 1–28.

Loisell, M.C., Wones, D.R., 1979. Charcteristics and origin of anorogranic granites. Geological Society of America Abstracts with Programs 11, 468.

Loizenbauer, J., Wallbrecher, E., Fritz, H., Neumayr, P., Khudeir, A.A., Kloetzli, U., 2001. Structural geology, single zircon ages and fluid inclusion studies of the Meatiq metamorphic core complex: Implications for Neoproterozoic tectonics in the Eastern Desert of Egypt. Precambrian Research 110, 357–383.

Lundmark, A.M., Andresen, A., Hassan, M.A., Augland, L.E., Abu El-Rus, M.A., Baghdady, G.Y., 2011, Repeated magmatic pulses in the East African Orogen of Central Eastern Desert, Egypt: an old idea supported by new evidence. Gondwana Research.

Lutz, T.M., Foland, K.A., Friedman, I., Serencsits, C.M., 1978. Ages of Egyptian alkaline complexes and Sr and O isotope relations at the Abu Khruq Complex. U.S. Geological Survey Open-File Report 78-101, pp. 265–267.

Malmgren, K., Andersson, W., 1994. Sukhaybarat gold mine. In: Collenette, P., Grainger, D.J. (Compilers), Mineral Resources of Saudi Arabia. Saudi Arabian Directorate General of Mineral Resources Special Publication DGMR-SP-2, pp. 111–115.

Martin, C., Roberts, R.J., Stoeser, D.B., 1979. Titaniferous Magnetite in the Layered Intrusive Complex at Lakathah, Kingdom of Saudi Arabia. USGS Saudi Project Report 238, 36 p.

Matsah, M., Kusky, T.M., 1999. Sedimentary facies of the Neoproterozoic Al-Jifn basin, NE Arabian shield: relationships to the Halaban-Zarghat (Najd) faults system and the closure of the Mozambique Ocean. In: Greiling, R. (Ed.), Pan-African of northern Africa–Arabia. Forschungszentrum Jülich. Geologisch-Palaeontoloigsches Institut, Ruprecht-Karls-Universitaet, Heidelberg, Proceedings of a Workshop, October 22–23, 1998.

Matsah, M.I.M., Kusky, T.M., 2001. Analysis of Landsat ratio imagery of the Halaban-Zarghat fault and related Jifn basin, NE Arabian shield: implications for the kinematic history of the Najd fault. Gondwana Research 4, 182.

Meert, J.G., 2002. A synopsis of events related to the assembly of eastern Gondwana. Tectonophysics 363, 1–40.

Meert, J.G., Lieberman, B.S., 2008. The Neoproterozoic assembly of Gondwana and its relationship to the Ediacaran–Cambrian radiation. Gondwana Research 14, 5–21.

Miller, M.M., Dixon, T.H., 1992. Late Proterozoic evolution of the N part of the Hamisana zone, NE Sudan: constraints on Pan-African accretionary tectonics. Journal of the Geological Society, London 149, 743–750.

Miller, N.R., Alene, M., Sacchi, R., Stern, R.J., Conti, A., Kröner, A., Zuppi, G., 2003. Significance of the Tambien Group (Tigrai, N. Ethiopia) for Snowball Earth events in the Arabian–Nubian Shield. Precambrian Research 121, 263–283.

Miller, N.R., Johnson, P.R., Stern, R.J., 2008. Marine versus non-marine environments for the Jibalah group, NW Arabian Shield: a sedimentologic and geochemical survey and report of possible metazoan in the Dhaiqa formation. Arabian Journal for Science and Engineering 33, 55–77.

Moghazi, A.M., Andersen, T., Oweiss, G.A., El-Bouseily, A.M., 1998. Geochemical and Sr–Nd–Pb isotopic data bearing on the origin of Pan-African granitoids in the Kid area, SE Sinai, Egypt. Journal of the Geological Society, London 155, 697–710.

Moghazi, A.M., Hassanen, M.A., Mohammed, F.H., Ali, S., 2004. Late Neoproterozoic strongly peraluminous leucogranites, South Eastern Desert, Egypt – petrogenesis and geodynamic significance. Mineralogy and Petrology 81, 19–41.

Mogren, S., Al-Amri, A.M., Al-Damegh, K., Faihead, D., Jassim, S., Algamdi, A., 2008. Sub-surface geometry of Ar Rika and Ruwah faults from gravity and magnetic surveys. Arabian Journal of Geosciences 1, 33–47.

Mohamed, F.H., Moghazi, A.M., Hassanen, M.A., 2000. Geochemistry, petrogenesis and tectonic setting of late Neoproterozoic Dokhan-type volcanic rocks in the Fatira area, eastern Egypt. International Journal of Earth Sciences 88, 764–777.

Möller, A., Mezger, K., Schenk, V., 1998. Crustal age domains and the evolution of the continental crust in the Mozambique Belt of Tanzania: Combined Sm–Nd, Rb–Sr, and Pb–Pb isotopic evidence. Journal of Petrology 39, 749–783.

Molnar, P., Tapponnier, P., 1977. Relation of the tectonics of eastern china to the India–Eurasia collision: application of slip-line field theory to large-scale continental tectonics. Geology 5, 212–216.

Moore, J.M., 1979. Tectonics of the Najd transcurrent fault system, Saudi Arabia. Journal of the Geological Society, London 136, 441–454.

Moufti, M.R.H., 2001. Age, geochemicstry, and origin of peraluminous A-type granitoids of the Ablah–Shuwas pluton, Ablah graben Arabian shield. Acta Mineralogica–Petrographica, Szeged 2001 42, 5–20.

Moussa, E.M.M., Stern, R.J., Manton, W.I., Ali, K.A., 2008. SHRIMP zircon dating and Sm/Nd isotopic investigations of Neoproterozoic granitoids, Eastern Desert, Egypt. Precambrian Research 160, 341–356.

Mushkin, A., Navon, O., Halitz, L., Heimann, A., Hartmann, G., Stein, M., 2003. The petrogenesis of A-type magmas from the Amram Massif, southern Israel. Journal of Petrology 44, 815–832.

Nawab, Z.A., 1979, Geology of the Al Amar-Idsas Region of the Arabian Shield. Evolution and Mineralization of the Arabian–Nubian Shield. King Abdulaziz University, Jeddah, Institute of Applied Geology Bulletin 3, v. 2, pp. 29–39.

Nettle, D., 2009. A Sequence Stratigraphic, Geochronological and Chemostratigraphic Investigation of the Ediacaran Antaq Basin, Eastern Arabian Shield, Saudi Arabia, Geology and Geophysics. University of Adelaide, p. 83.

Neumayr, P., Mogessie, A., Hoinkes, G., Puhl, J., 1996a. Geological setting of the Meatiq metamorphic core complex in the Eastern Desert of Egypt based on amphibolite geochemistry. Journal of African Earth Sciences 23, 331–345.

Neumayr, P., Hoinkes, G., Puhl, J., Mogessie, A., 1996b. Polymetamorphism in the Meatiq basement complex (Eastern Desert, Egypt): P – T variations and implications for tectonic evolution. Geological Survey of Egypt, Centennial Symposium Abstracts, pp. 139–141.

Neumayr, P., Hoinkes, G., Puhl, J., Mogessie, A., Khudeir, A.A., 1998. The Meatiq Dome, (Eastern Desert, Egypt) a Precambrian metamorphic core complex: petrological and geological evidences. Journal of Metamorphic Geology 16, 259–279.

Nicholson, P.G., Janjou, D., Fanning, C.M., Heaman, L.M., Grotzinger, J.P., 2008. Deposition, age and Pan-African correlation of late Neoproterozoic outcrops in Saudi Arabia. In: Geo 2008: 8th Middle East Geoscience Conference and Exhibition, Manama, Bahrain, March 2–5, 2008.

Passchier, C., 2010. The Al Wajh shear zone system, NW Saudi Arabia. In: Pease, V., Kadi, K.A., Kozdroj, W. (Eds.), JEBEL Project October 2009 Field Excursion to the Midyan Terrane, Kingdom of Saudi Arabia with Reports on Research by Participants of the JEBEL Project. Saudi Geological Survey Technical Report SGS-TR-2010-2, pp. 76–77.

Pearce, J.A., 1996. Sources and settings of granitic rocks. Episodes 19, 120–125.

Pearce, J.A., Harris, N.B.W., Tindle, A.G., 1984. Trace element discrimination diagrams for the tectonic interpretation of granitic rocks. Journal of Petrology 25, 956–983.

Pellaton, C., 1985. Geologic Map of the Miskah Quadrangles, Sheet 24F, Kingdom of Saudi Arabia. Saudi Arabian Deputy Ministry for Mineral Resources Geoscience Map GM-99, Scale 1:250,000, 23 p.

Pisarevsky, S.A., Murphy, J.B., Cawood, P.A., Collins, A.S., 2008. Late Neoproterozoic and Early Cambrian palaeogeography: models and problems. In: Brito Neves, B.B., Trouw, R.A.J., de Wit, M.J., Pankhurst, R.J. (Eds.), Western Gondwana: Pre-Cenozoic Geology Bordering the S Atlantic. Geological Society, London, Special Publication, pp. 9–32.

Plimer, I.R., 1987. Fundamental parameters for the formation of granite-related tin deposits. Geologische Rundschau 76, 23–40.

Pouit, G., Elsass, P., Ferrand, A., Milesi, J.P., Sabir, H., 1984. Metallogenic Base Metal Studies: Review of Activity during 1980–1983 AD (1400–1403 A.H.). Saudi Arabian Deputy Ministry for Mineral Resources Open-File Report BRGM-OF-04-11, 74 p.

Raharimahefa, T., Kusky, T.M., 2006. Structural and remote sensing studies of the southern Betsisimarka suture, Madagascar. Gondwana Research 10, 186–197.

Raharimahefa, T., Kusky, T.M., 2010. Temporal evolution of the Angavo and related shear zones in Gondwana. Constraints from LAMC-ICP-MS-U–PB zircon ages of granitoids and gneiss from central Madagascar. Precambrian Research 182, 30–42. doi:10.1016/j.precamres.2010.06.013.

Ramsay, C.R., 1986. Specialized felsic plutonic rocks of the Arabian Shield and their precursors. Journal of African Earth Sciences 4, 153–168.

Ramsay, C.R., Stoeser, D.B., Drysdall, A.R., 1986. Guide lines to classification and nomenclature of Arabian felsic plutonic rocks. Journal of African Earth Sciences 4, 13–20.

Renne, P.R., Mundil, R., Balco, G., Min, K., Ludwig, K.R., 2010. Joint determination of ^{40}K decay constants and ^{40}Ar/^{40}K for the Fish canyon sanidine standard, and improved accuracy for ^{40}Ar/^{39}Ar geochronology. Geochimica et Cosmochimica Acta 74, 5349–5367.

Ressetar, R., Monrad, J.R., 1983. Chemical composition and tectonic setting of the Dokhan Volcanic formation, Eastern Desert, Egypt. Journal of African Earth Sciences 1, 103–112.

Reymer, A.P.S., Matthews, A., Navon, O., 1984. Pressure–temperature conditions in the Wadi Kid metamorphic complex: implications for the Pan-African event in SE Sinai. Contributions to Mineralogy and Petrology 85, 336–345.

Rice, A.H.N., Greiling, R.O., Dardir, A.A., Rashwan, A.A., Sadek, M.F., 1992. Pan-African extensional structures in the area S of the Hafafit Antiform, Eastern Desert of Egypt. Zentralblatt fur Geologie und Palaeontolgie Teil I 11, 2641–2651.

Ries, A.C., Shackleton, R.M., Graham, R.H., Fitches, W.R., 1983. Pan African structures, ophiolites and mélange in the Eastern Desert of Egypt. A traverse at 26°N. Journal of the Geological Society, London 140, 75–95.

Ries, A.C., Shackleton, R.M., Dawoud, A.S., 1985. Geochronology, geochemistry, and tectonics of the NE Bayuda Desert, N. Sudan–implications for the western margin of the late Proterozoic fold belt of NW Africa. Precambrian Research 30, 43–62.

Ring, U., Brandon, M.T., Willet, S.D., Lister, G.S., 1999. Exhumation processes. In: Ring, U., Grandon, M.T., Lister, G.S., Willet, S.D. (Eds.), Exhumation Processes. Normal Faulting, Ductile Flow and Erosion. Geological Society, London, Special Publication, 154, pp. 1–27.

Sadek, M.F., 1994. A structural synthesis of the Proterozoic Arabian-Shield in Egypt. Geologische Rundschau 83, 484–501.

Samuel, M.D., Moussa, H.E., Azer, M.K., 2007. A-type volcanics in central eastern Sinai, Egypt. Journal of African Earth Sciences 47, 203–226.

Sangster, D.F., Abdulhay, G.J.S., 2005, Base metal (Cu–Pb–Zn) mineralization in the Kingdom of Saudi Arabia: Saudi Geological Survey (Jeddah), 128 p.

Schandelmeier, H., Abdel Rahman, E.M., Wipfler, E., Küster, D., Utke, A., Matheis, G., 1994. Late Proterozoic magmatism in the Nakasib suture, Red Sea Hills, Sudan. Journal of the Geological Society, London 151, 485–497.

Schmidt, D.L., 1981. Geology of the Jabal Yafikh Quadrangle, Sheet 23/43B, Kingdom of Saudi Arabia. US Geological Survey Saudi Arabian Mission Miscellaneous Documents 39, Scale 1:100,000, 99 p.

Schmidt, D.L., Hadley, D.G., Stoeser, D.B., 1979. Late Proterozoic crustal history of the Arabian shield, southern Najd province, Kingdom of Saudi Arabia. King Abdulaziz University, Jiddah. Institute of Applied Geology Bulletin 3 (2), 41–58.

Sengör, A.M.C., Natalin, B.A., 1996. Paleotectonics of Asia: fragment of a synthesis. In: Yin, A., Harrison, T.M. (Eds.), The Tectonics of Asia. Cambridge University Press, New York, pp. 486–640.

Shackleton, R.M., 1994. Review of Late Proterozoic sutures, ophiolite melanges and tectonics of eastern Egypt and NE Sudan. Geologische Rundschau 83, 537–546.

Shalaby, A., 2010. The northern dome of Wadi Hafafit culmination, Eastern Desert, Egypt: structural setting in tectonic framework of a scissor-like wrench corridor. Journal of African Earth Sciences 57, 227–241.

Shalaby, A., Stüwe, K., Makroum, F., Frtiz, H., Kebede, T., Klötzli, U., 2005. The Wadi Mubarak belt, Eastern Desert of Egypt: a Neoproterozoic conjugate shear system in the Arabian–Nubian Shield. Precambrian Research 136, 27–50.

Shalaby, A., Stüwe, K., Fritz, H., Makroum, F., 2006. The El Mayah molasse basin in the Eastern Desert of Egypt. Journal of African Earth Sciences 45, 1–15.

Sharland, P.R., Archer, R., Casey, D.M., Davies, R.B., Hall, S.H., Heward, A.P., Horbury, A.D., Simmons, M.D., 2001. Arabian Plate Sequence Stratigraphy. GeoArabia Special Publication 2, 371 p.

Shimron, A.E., 1984. Evolution of the Kid Group, SE Sinai Peninsula: thrusts, mélange and implications for accretionary tectonics during Late Proterozoic of the Arabian–Nubian Shield. Geology 12, 242–247.

Shimron, A.E., 1987. Pan-African metamorphism and deformation in the Wadi Kid region, SE Sinai Peninsula: evidence from porphyroblasts in the Umm Zariq Formation. Israel Journal of Earth Sciences 36, 173–193.

Shimron, A.E., 1990. The Red Sea line – a late-Proterozoic transcurrent fault. Journal of African Earth Sciences 11, 95–112.

Sibson, R.H., 1987. Earthquake rupturing as a mineralizing agent in hydrothermal systems. Geology 15, 701–704.

Smith, A.G., 2009. Neoproterozoic timescales and stratigraphy. In: Craig, J., Thurow, J., Thusu, B., Whitham, A., Abutarrama, Y. (Eds.), Global Neoproterozoic Petroleum Systems: The Emerging Potential in N Africa. Geological Society, vol. 326, London, Special Publication, pp. 27–54. doi: 10.1144/SP326.2.

Smith, M., O'Conner, E., Nasr, B.B., 1998. Transpressional flower structures and escape tectonics: a new look at the Pan-African collision in the Eastern Desert, Egypt. In: Greiling, R.O. (Ed.), Workshop on the Pan-African of Northern Africa–Arabia, Geologisch-Palaeontologiches Institut, Ruprecht-Karls Universitaet, Heidelberg Germany, October 22–23.

Squire, R.J., Campbell, I.H., Allen, C.M., Wilson, C.J.L., 2006. Did the Transgondwanan Supermountain trigger the explosive radiation of animals on Earth? Earth and Planetary Science Letters 250, 116–133.

SRK Consulting, 2007. An independent Mineral Experts' Report on the Gold Mining and Exploration Assets of Saudi Arabian Mining Company (Ma'aden). SRK Consulting Engineers and Scientists, Cardiff, 315 p (available on Ma'aden website).

Stacey, J.S., Agar, R.A., 1985. U–Pb isotopic evidence for the accretion of a continental micro plate in the Zalm region of the Saudi Arabian Shield. Journal of the Geological Society, London 142, 1189–1203.

Stacey, J.S., Hedge, C.E., 1984. Geochronologic and isotopic evidence for early Proterozoic crust in the eastern Arabian Shield. Geology 12, 310–313.

Stacey, J.S., Stoeser, D.B., 1984. Distribution of oceanic and continental leads in the Arabian–Nubian Shield. Contributions to Mineralogy and Petrology 54, 91–105.

Stacey, J.S., Doe, B.R., Roberts, R.J., Delevaux, M.H., Gramlich, J.W., 1980. Lead isotope study of mineralization in the Saudi Arabian shield. Contributions to Mineralogy and Petrology 74, 175–188.

Stacey, J.S., Stoeser, D.B., Greenwood, W.R., Fischer, L.B., 1984. U–Pb zircon geochronology and geologic evolution of the Halaban–Al Amar region of the eastern Arabian Shield, Kingdom of Saudi Arabia. Journal of the Geological Society, London 141, 1043–1055.

Stern, R.J., 1979. Late Precambrian Ensimatic Volcanism in the Central Eastern Desert of Egypt. Ph.D. Thesis, University of California, San Diego, 210 p.

Stern, R.J., 1985. The Najd fault system, Saudi Arabia and Egypt: a late Precambrian rift-related transform system? Tectonics 4, 497–511.

Stern, R.J., 1994. Arc assembly and continental collision in the Neoproterozoic East African Orogen: implications for the consolidation of Gondwanaland. Annual Reviews of Earth and Planetary Sciences 22, 315–319.

Stern, R.J., 2002. Crustal evolution in the East African Orogen: a neodymium isotopic perspective. Journal of African Earth Sciences 34, 109–117.

Stern, R.J., Abdelsalam, M.G., 1998. Formation of juvenile continental crust in the Arabian–Nubian shield: evidence from granitic rocks of the Nakasib Suture, NE Sudan. Geologische Rundschau 87, 150–160.

Stern, R.J., Gottfried, D., 1986. Petrogenesis of a Late Precambrian (575–600 Ma) bimodal suite in the N Eastern Desert of Egypt. Contributions to Mineralogy and Petrology 92, 492–501.

Stern, R.J., Hedge, C.E., 1985. Geochronologic and isotopic constraints on late Precambrian crustal evolution in the Eastern Desert of Egypt. American Journal of Science 285, 97–172.

Stern, R.J., Johnson, P.R., 2010. Continental lithosphere of the Arabian Plate: a geologic, petrologic, and geophysical synthesis. Earth-Science Reviews 101, 29–67.

Stern, R.J., Manton, W.I., 1987. Age of Feiran basement rocks, Sinai – implications for late Precambrian crustal evolution in the northern Arabian–Nubian Shield. Journal of the Geological Society, London 144, 569–575.

Stern, R.J., Voegeli, D.A., 1987. Geochemistry, geochronology, and petrogenesis of a late Precambrian (590 Ma) composite dike from the N Eastern Desert of Egypt. Geologische Rundschau 76, 325–341.

Stern, R.J., Gottfried, D., Hedge, C.E., 1984. Late Precambrian rifting and crustal evolution in the northeastern Desert of Egypt. Geology 12, 168–172.

Stern, R.J., Kröner, A., Manton, W.I., Reischmann, T., Mansour, M., Hussein, I.M., 1989. Geochronology of the late Precambrian Hamisana shear zone, Red Sea

Hills, Sudan and Egypt. Journal of the Geological Society, London 146, 1017–1029.
Stern, R.J., Ali, K.A., Andresen, A., Wilde, S., Abu-El-Ene, M., Hassan, I., 2010a. Results of Geochronological Investigations in Sinai Undertaken as Part of the 2008 JEBEL Field Trip. Saudi Geological Survey Technical Report – SGS-TR-2010-2, pp. 46–51.
Stern, R.J., Ali, K.A., Liégeois, J.-P., Johnson, P., Wiescek, F., Kattan, F., 2010b. Distribution and significance of pre-Neoproterozoic zircons in juvenile Neoproterozoic igneous rocks of the Arabian–Nubian Shield. American Journal of Science 310, 791–811.
Stockli, D.F., 2005. Application of low-temperature thermochronometry to extensional tectonic settings. Review in Mineralogy and Geochemistry 58, 411–448.
Stoeser, D.B., 1986. Distribution and tectonic setting of plutonic rocks of the Arabian Shield. Journal of African Earth Sciences 4, 21–46.
Stoeser, D.B., Camp, E., 1985. Pan-African microplate accretion of the Arabian shield. Geological Society of America Bulletin 96, 817–826.
Stoeser, D.B., Frost, C.D., 2006. Nd, Pb, Sr, and O isotopic characteristics of Saudi Arabian shield terranes. Chemical Geology 226, 163–188.
Stoeser, D.B., Stacey, J.S., 1988. Evolution, U–Pb geochronology, and isotope geology of the Pan-African Nabitah orogenic belt of the Saudi Arabian Shield. In: El-Gaby, S., Greiling, R.O. (Eds.), The Pan-African belt of NE African and Adjacent Areas. Friedrich, Viewig and Sohn, Braunschweig/Wiesbaden, pp. 227–288.
Stoeser, D.B., Whitehouse, M.J., Stacey, J.S., 2001. The Khida terrane – geology of Paleoproterozoic rocks in the Muhayil area, eastern Arabian shield, Saudi Arabia. Gondwana Research 4, 192–194.
Streckeisen, A., 1976. To each plutonic rock its proper name. Earth Science Reviews 12, 1–33.
Sturchio, N.C., Sultan, M., Batiza, R., 1983a. Geology and origin of Meatiq Dome, Egypt: a Precambrian metamorphic core complex? Geology 11, 72–76.
Sturchio, N.C., Sultan, M., Sylvester, P., Batiza, R., Hedge, C., El Shazly, E.M., Abdel-Maguid, A., 1983b. Geology, age, and origin of the Meatiq Dome – implications for the Precambrian stratigraphy and tectonic evolution of the Eastern Desert of Egypt. King Abdulaziz University, Faculty of Earth Sciences Bulletin 6, 127–143.
Sultan, M., Arvidson, R.E., Duncan, I.J., Stern, R., El Kaliouby, B., 1988. Extension of the Najd Fault System from Saudi Arabia to the central Eastern Desert of Egypt based on integrated field and Landsat observations. Tectonics 7, 1291–1306.
Tadesse, T., 1996. Structure across a possible intra-oceanic suture zone in the low-grade Pan-African rocks of northern Ethiopia. Journal of African Earth Sciences 23, 375–381.
Tadesse, S., Milesi, J.-P., Deschamps, Y., 2003. Geology and mineral potential of Ethiopia: a note on geology and mineral map of Ethiopia. Journal of African Earth Sciences 36, 273–313.
Tapponnier, P., Molnar, P., 1976. Slip-line field theory and large-scale continental tectonics. Nature 264, 319–324.
Teklay, M., Kröner, A., Mezger, K., 2001. Geochemistry, geochronology, and isotope geology of Nakfa intrusive rocks, northern Eritrea: products of a tectonically thickened Neoproterozoic arc crust. Journal of African Earth Sciences 3 (33), 283–301.
Tenczer, V., Hauzenberger, C.A., Fritz, H., Whitehouse, M.J., Mogessie, A., Wallbrecher, E., Muhongo, S., Hoinkes, G., 2006. ANosites in the Eastern Granulites of Tanzania—new SIMS zircon U–Pb age data, petrography and geochemistry. Precambrian Research 148, 85–114.
Testard, J., 1983. Khnaiguiyah, a Synsedimentary Hydrothermal Deposit Comprising Cu–Zn–Fe Sulfides and Fe Oxides in an Ignimbritic Setting. Saudi Arabian Deputy Ministry for Mineral Resources Open-File Report BRGM-OF-03-9, 106 p.
Tsige, L., Abdelsalam, M.G., 2005. Neoproterozoic–Early Paleozoic gravitational tectonic collapse in the southern part of the Arabian–Nubian Shield. The Bulbul Belt of southern Ethiopia. Precambrian Research 138, 297–318.
Vickers-Rich, P., Kozdroj, W., Kattan, F.H., Leonov, M., Ivantsov, A., Johnson, P.R., et al., 2010. Reconnaissance for an Ediacaran Fauna, Kingdom of Saudi Arabia. Saudi Arabian Geological Survey Technical Report SGS-TR-2010-8, 42 p.
Volesky, J.C., Stern, R.J., Johnson, P.R., 2003. Geological control of massive sulfide mineralization in the Neoproterozoic Wadi Bidah shear zone, southwestern Saudi Arabia, inferences from orbital remote sensing and field studies. Precambrian Research 123, 235–247.
Walker, B.M., Lewis, R.S., Al Otaibi, R. Ben Talib, M. Christian, R., Gabriel, B.R., 1994. An Najadi Gold Prospect, Kingdom of Saudi Arabia; Geology and Gold-resource Assessment. Saudi Arabian Deputy Ministry for Mineral Resources Technical Report USGS-TR-94-5, 89 p.
Wallace, C.A., 1986. Lithofacies and Depositional Environment of the Maraghan Formation, and Speculation on the Origin of Gold in Ancient Mines, an Najadi area, Kingdom of Saudi Arabia. Saudi Arabian Deputy Ministry for Mineral Resources Open-File Report USGS-OF-06-6.19 p.
Whitehouse, M.J., Windley, B.F., Ba-Bttat, M.A.O., Fanning, C.M., Rex, D.C., 1998. Crustal evolution and terrane correlation in the eastern Arabian shield, Yemen: Geochronologic constraints. Journal of the Geological Society, London 155, 281–295.
Whitehouse, M.J., Stoeser, D.B., Stacey, J.S., 2001. The Khida Terrane–Geochronological and isotopic evidence for Paleoproterozoic and Archean crust in the eastern Arabian shield of Saudi Arabia. Gondwana Research 4, 200–202.
Wilde, S.A., Youssef, K., 2000. Significance of SHRIMP U–Pb dating of the imperial Porphyry and associated Dokhan Volcanics, Gebel Dokhan, N Eastern Desert, Egypt. Journal of African Earth Sciences 31, 410–413.
Wilde, S.A., Youssef, K., 2002. A re-evaluation of the origin and setting of the Late Precambrian Hammamat Group based on SHRIMP U-Pb dating of detrital zircons from Gebel Umm Tawat, North Eastern Desert, Egypt. Journal of the Geological Society, London 159, 595–604.
Williams, P.L., Vaslet, D., Johnson, P.R., Berthiaux, A., Le Strat, P., Fourniguet, J., 1986. Geologic Map of the Jabal Hibshi Quadrangle, Sheet 26F, Kingdom of Saudi Arabia. Saudi Arabian Deputy Ministry for Mineral Resources Geoscience Map GM-98, Scale 1:250,000, 52 p.
Willis, K.M., Stern, R.J., Clauer, N., 1988. Age and geochemistry of late Precambrian sediments of the Hammamat series from the northeastern desert of Egypt. Precambrian Research 42, 173–187.
Windley, B.F., Whitehouse, M.J., Ba-Bttat, M.A.O., 1996. Early Precambrian gneiss terranes and Pan-African island arcs in Yemen: crustal accretion of the eastern Arabian Shield. Geology 24, 131–134.
Worku, H., Schandelmeier, H., 1996. Tectonic evolution of the Neoproterozoic Adola Belt of southern Ethiopia: evidence for a Wilson cycle process and implications for oblique plate collision. Precambrian Research 77, 179–210.
Yibas, B., Reimold, W.U., Armstrong, R., Koeberl, C., Anhaeusser, C.R., Phillips, D., 2002. The tectonostratigraphy, granitoid geochronology and geological evolution of the Precambrian of southern Ethiopia. Journal of African Earth Sciences 34, 57–84.
Yihunie, T., Tesfaye, M., 2002. Structural evidence for the allochthonous nature of the Balbul terrane in southern Ethiopia: A west-verging thrust nappe. Journal of African Earth Sciences 34, 85–93.
Youssef, K.M., 2005. The Age and Petrogenesis of the Major Rock Units at Gabal Gattar and Gabal El Dokhan, Northeastern Desert, Egypt. Unpublished PhD Thesis, Curtin University of Technology, 298 p.
Zahran A.M., Stewart, I.C.F., Johnson, P.R., Basahel, M.H., 2003. Aeromagnetic-anomaly maps of central and western Saudi Arabia. Saudi Geological Survey Open-File Report SGS-OF-2002-8, scale 1:2,000,000.
Zoheir, B.A., Akawy, A., 2010. Genesis of the Abu Marawat gold deposit, central Eastern Desert of Egypt. Journal of African Earth Sciences 57, 306–320.